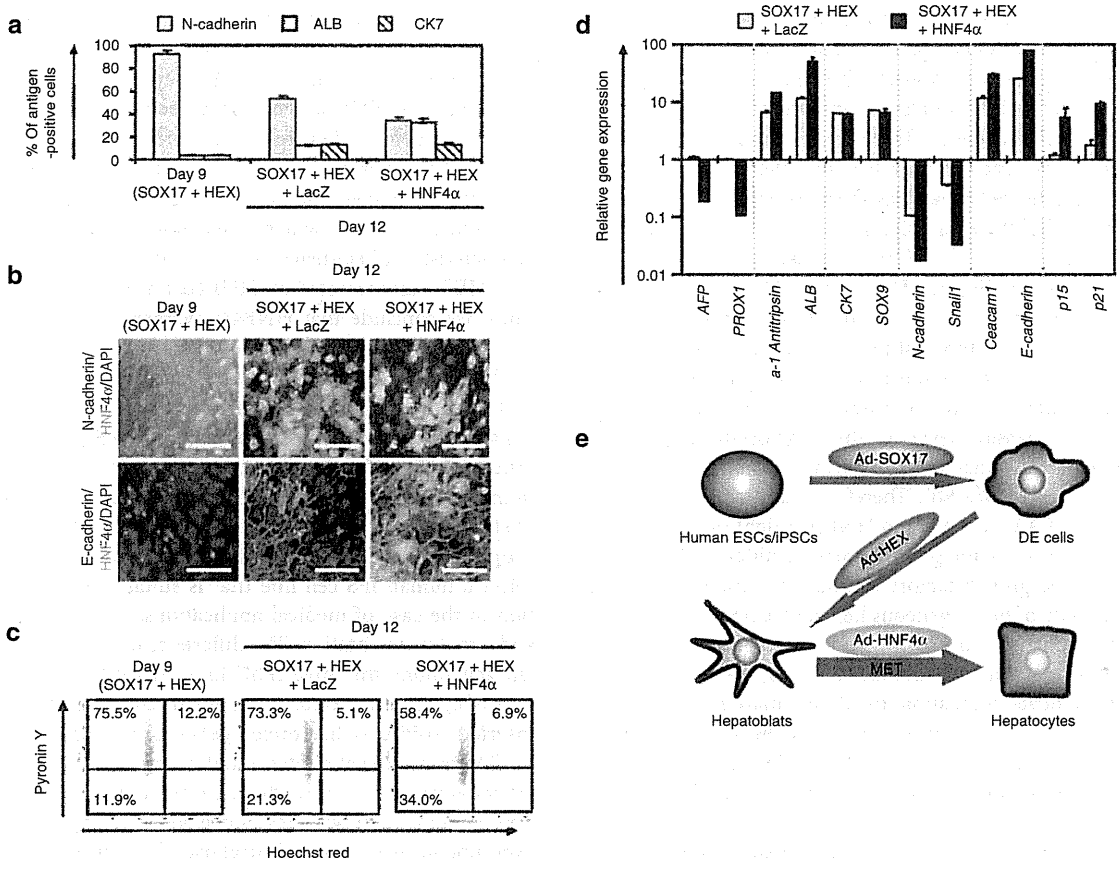

Figure 5 HNF4α promotes hepatic differentiation by activating MET. Human ESCs were differentiated into hepatoblasts according to the protocol described in **Figure 2a**, and then transduced with 3,000 VP/cell of Ad-LacZ or Ad-HNF4α for 1.5 hours, and finally cultured until day 12 of differentiation. (**a**) The hepatoblasts, two factors plus Ad-LacZ-transduced cells (SOX17+HEX+LacZ) (day 12), and the three factors-transduced cells (SOX17+HEX+HNF4α) (day 12) were subjected to immunostaining with anti-N-cadherin, ALB, or CK7 antibodies. The percentage of antigen-positive cells was measured by flow cytometry. (**b**) The cells were subjected to immunostaining with anti-N-cadherin (green), E-cadherin (green), or HNF4α (red) antibodies on day 9 or day 12 of differentiation. Nuclei were counterstained with DAPI (blue). The bar represents 50 μm. Similar results were obtained in two independent experiments. (**c**) The cell cycle was examined on day 9 or day 12 of differentiation. The cells were stained with Pyronin Y (y-axis) and Hoechst 33342 (x-axis) and then analyzed by flow cytometry. The growth fraction of cells is the population of actively dividing cells (G1/S/G2/M). (**d**) The expression levels of *AFP*, *PROX1*, *α-1-antitrypsin*, *ALB*, *CK7*, *SOX9*, *N-cadherin*, *Snail1*, *Ceacam1*, *E-cadherin*, *p15*, and *p21* were examined by real-time RT-PCR on day 9 or day 12 of differentiation. The expression level of hepatoblasts (day 9) was taken as 1.0. All data are represented as means ± SD ($n = 3$). (**e**) The model of efficient hepatic differentiation from human ESCs and iPSCs in this study is summarized. The human ESCs and iPSCs differentiate into hepatocytes via definitive endoderm and hepatoblasts. At each stage, the differentiation is promoted by stage-specific transduction of appropriate functional genes. In the last stage of hepatic differentiation, HNF4α transduction provokes hepatic maturation by activating MET. ESC, embryonic stem cell; HNF4α, hepatocyte nuclear factor 4α; iPSC, induced pluripotent stem cell; MET, mesenchymal-to-epithelial transition; RT-PCR, reverse transcription-PCR; VP, vector particle.

The gene expression levels of hepatocyte markers (*α-1-antitrypsin* and *ALB*)[20] and epithelial markers (*Ceacam1* and *E-cadherin*) were upregulated by HNF4α transduction. On the other hand, the gene expression levels of hepatoblast markers (*AFP* and *PROX1*)[31], mesenchymal markers (*N-cadherin* and *Snail*)[32], and cyclin dependent kinase inhibitor (*p15* and *p21*)[33] were downregulated by HNF4α transduction. HNF4α transduction did not change the expression levels of cholangiocyte markers (*CK7* and *SOX9*). We conclude that HNF4α promotes hepatic maturation by activating MET.

DISCUSSION

This study has two main purposes: the generation of functional hepatocytes from human ESCs and iPSCs for application to drug toxicity screening in the early phase of pharmaceutical development and; elucidation of the HNF4α function in hepatic maturation from human ESCs. We initially confirmed the importance of transcription factor HNF4α in hepatic differentiation from human ESCs by using a published data set of gene array analysis (**Supplementary Figure S1**).[34] We speculated that HNF4α transduction could enhance hepatic differentiation from human ESCs and iPSCs.

To generate functional hepatocytes from human ESCs and iPSCs and to elucidate the function of HNF4α in hepatic differentiation from human ESCs, we examined the stage-specific roles of HNF4α. We found that hepatoblast (day 9) stage-specific HNF4α transduction promoted hepatic differentiation (**Figure 1**). Because endogenous HNF4α is initially expressed in the hepatoblast,[9,10] our system might adequately reflect early embryogenesis. However, HNF4α transduction at an inappropriate stage (day 6 or day 12) promoted

bidirectional differentiation; heterogeneous populations, which contain the hepatocytes and pancreas cells or hepatocytes and cholangiocytes, were obtained, respectively (**Figure 1**), consistent with a previous report that HNF4α plays an important role not only in the liver but also in the pancreas.[12] Therefore, we concluded that HNF4α plays a significant stage-specific role in the differentiation of human ESC- and iPSC-derived hepatoblasts to hepatocytes (**Figure 5e**).

We found that the expression levels of the hepatic functional genes were upregulated by HNF4α transduction (**Figure 3a,b**, and **Supplementary Figures S7** and **S8**). Although the c/EBPα and GATA4 expression levels of the three factors-transduced cells were higher than those of primary human hepatocytes, the FOXA1, FOXA2, FOXA3, and HNF1α, which are known to be important for hepatic direct reprogramming and hepatic differentiation,[35,36] expression levels of three factors-transduced cells were slightly lower than those of primary human hepatocytes (**Supplementary Figure S8**). Therefore, additional transduction of FOXA1, FOXA2, FOXA3, and HNF1α might promote further hepatic maturation. Some previous hepatic differentiation protocols that utilized growth factors without gene transfer led to the appearance only of heterogeneous hepatocyte populations.[4–6] The HNF4α transduction led not only to the upregulation of expression levels of several hepatic markers but also to an almost homogeneous hepatocyte population; the differentiation efficacy based on CYPs, ASGR1, or ALB expression was ~80% (**Figure 3c–e**). The efficient hepatic maturation in this study might be attributable to the activation of many hepatocyte-associated genes by the transduction of HNF4α, which binds to the promoters of nearly half of the genes expressed in the liver.[12] In the later stage of hepatic maturation, hepatocyte-associated genes would be strongly upregulated by endogenous transcription factors but not exogenous HNF4α because transgene expression by Ad vectors was almost disappeared on day 18 (**Supplementary Figure S5**). Another reason for the efficient hepatic maturation would be that sequential transduction of SOX17, HEX, and HNF4α could mimic hepatic differentiation in early embryogenesis.

Next, we examined whether or not the hepatocyte-like cells had hepatic functions. The activity of many kinds of CYPs was upregulated by HNF4α transduction (**Figure 4b**). Ad-HNF4α-transduced cells exhibit many characteristics of hepatocytes: uptake of LDL, uptake and excretion of ICG, and storage of glycogen (**Figure 4a,c,d**). Many conventional tests of hepatic characteristics have shown that the hepatocyte-like cells have mature hepatocyte functions. Furthermore, the hepatocyte-like cells can catalyze the toxication of several compounds (**Figure 4e**). Although the activities to catalyze the toxication of test compounds in primary human hepatocytes are slightly higher than those in the hepatocyte-like cells, the handling of primary human hepatocytes is difficult for a number of reasons: since their source is limited, large-scale primary human hepatocytes are difficult to prepare as a homogeneous population. Therefore, the hepatocyte-like cells derived from human ESCs and iPSCs would be a valuable tool for predicting drug toxicity. To utilize the hepatocyte-like cells in a drug toxicity study, further investigation of the drug metabolism capacity and CYP induction potency will be needed.

We also investigated the mechanisms underlying efficient hepatic maturation by HNF4α transduction. Although the number of cholangiocyte populations did not change by HNF4α transduction, we found that the number of hepatoblast populations decreased and that of hepatocyte populations increased, indicating that HNF4α promotes selective hepatic differentiation from hepatoblasts (**Figure 5a**). As previously reported, HNF4α regulates the expression of a broad range of genes that code for cell adhesion molecules,[13] extracellular matrix components, and cytoskeletal proteins, which determine the main morphological characteristics of epithelial cells.[14,35,37] In this study, we elucidated that MET was promoted by HNF4α transduction (**Figure 5b,d**). Thus, we conclude that HNF4α overexpression in hepatoblasts promotes hepatic differentiation by activating MET (**Figure 5e**).

Using human iPSCs as well as human ESCs, we confirmed that the stage-specific overexpression of HNF4α could promote hepatic maturation (**Supplementary Figure S9**). Interestingly, the differentiation efficacies differed among human iPS cell lines: two of the human iPS cell lines (Dotcom and Tic) were more committed to the hepatic lineage than another human iPS cell line (201B7) (**Supplementary Figure S7**). Therefore, it would be necessary to select a human iPS cell line that is suitable for hepatic maturation in the case of medical applications, such as drug screening and liver transplantation. The difference of hepatic differentiation efficacy among the three iPSC lines might be due to the difference of epigenetic memory of original cells or the difference of the inserted position of the foreign genes for the reprogramming.

To control hepatic differentiation mimicking embryogenesis, we employed Ad vectors, which are one of the most efficient transient gene delivery vehicles and have been widely used in both experimental studies and clinical trials.[38] We used a fiber-modified Ad vector containing the EF-1α promoter and a stretch of lysine residue (KKKKKKK, K7) peptides in the C-terminal region of the fiber knob.[19] The K7 peptide targets heparan sulfates on the cellular surface, and the fiber-modified Ad vector containing the K7 peptides was shown to be efficient for transduction into many kinds of cells including human ESCs and human ESC-derived cells.[7–8,19] Thus, Ad vector-mediated transient gene transfer should be a powerful tool for regulating cellular differentiation.

In summary, the findings described here demonstrate that transcription factor HNF4α plays a crucial role in the hepatic differentiation from human ESC-derived hepatoblasts by activating MET (**Figure 5e**). In the present study, both human ESCs and iPSCs (three lines) were used and all cell lines showed efficient hepatic maturation, indicating that our protocol would be a universal tool for cell line-independent differentiation into functional hepatocytes. Moreover, the hepatocyte-like cells can catalyze the toxication of several compounds as primary human hepatocytes. Therefore, our technology, by sequential transduction of SOX17, HEX, and HNF4α, would be a valuable tool for the efficient generation of functional hepatocytes derived from human ESCs and iPSCs, and the hepatocyte-like cells could be used for the prediction of drug toxicity.

MATERIALS AND METHODS

Human ESC and iPSC culture. A human ES cell line, H9 (WiCell Research Institute, Madison, HI), was maintained on a feeder layer of mitomycin C-treated mouse embryonic fibroblasts (Millipore, Billerica, MA) with Repro Stem (Repro CELL, Tokyo, Japan) supplemented with 5 ng/ml fibroblast

growth factor 2 (FGF2) (Sigma, St Louis, MO). Human ESCs were dissociated with 0.1 mg/ml dispase (Roche Diagnostics, Indianapolis, IN) into small clumps and then were subcultured every 4 or 5 days. H9 was used following the Guidelines for Derivation and Utilization of Human Embryonic Stem Cells of the Ministry of Education, Culture, Sports, Science and Technology of Japan. Two human iPS cell lines generated from the human embryonic lung fibroblast cell line MCR5 were provided from the JCRB Cell Bank (Tic, JCRB Number: JCRB1331; and Dotcom, JCRB Number: JCRB1327).[39,40] These human iPS cell lines were maintained on a feeder layer of mitomycin C-treated mouse embryonic fibroblasts with iPSellon (Cardio, Kobe, Japan) supplemented with 10 ng/ml FGF2. Another human iPS cell line, 201B7, generated from human dermal fibroblasts was kindly provided by Dr S. Yamanaka (Kyoto University).[2] The human iPS cell line 201B7 was maintained on a feeder layer of mitomycin C-treated mouse embryonic fibroblasts with Repro Stem (Repro CELL) supplemented with 5 ng/ml FGF2 (Sigma). Human iPSCs were dissociated with 0.1 mg/ml dispase (Roche Diagnostics) into small clumps and were then subcultured every 5 or 6 days.

In vitro *differentiation.* Before the initiation of cellular differentiation, the medium of human ESCs and iPSCs was exchanged for a defined serum-free medium, hESF9, and cultured as we previously reported.[41] hESF9 consists of hESF-GRO medium (Cell Science & Technology Institute, Sendai, Japan) supplemented with 10 μg/ml human recombinant insulin, 5 μg/ml human apotransferrin, 10 μmol/l 2-mercaptoethanol, 10 μmol/l ethanolamine, 10 μmol/l sodium selenite, oleic acid conjugated with fatty-acid-free bovine albumin (BSA), 10 ng/ml FGF2, and 100 ng/ml heparin (all from Sigma).

The differentiation protocol for the induction of DE cells, hepatoblasts, and hepatocytes was based on our previous report with some modifications.[7] Briefly, in mesendoderm differentiation, human ESCs and iPSCs were dissociated into single cells and cultured for 3 days on Matrigel (Becton, Dickinson and Company, Tokyo, Japan) in hESF-DIF medium (Cell Science & Technology Institute) supplemented with 10 μg/ml human recombinant insulin, 5 μg/ml human apotransferrin, 10 μmol/l 2-mercaptoethanol, 10 μmol/l ethanolamine, 10 μmol/l sodium selenite, 0.5 mg/ml BSA, and 100 ng/ml Activin A (R&D Systems, Minneapolis, MN). To generate mesendoderm cells and DE cells, human ESC-derived cells were transduced with 3,000 vector particles (VP)/cell of Ad-SOX17 for 1.5 hours on day 3 and cultured until day 6 on Matrigel (BD) in hESF-DIF medium (Cell Science & Technology Institute) supplemented with 10 μg/ml human recombinant insulin, 5 μg/ml human apotransferrin, 10 μmol/l 2-mercaptoethanol, 10 μmol/l ethanolamine, 10 μmol/l sodium selenite, 0.5 mg/ml BSA, and 100 ng/ml Activin A (R&D Systems). For induction of hepatoblasts, the DE cells were transduced with 3,000 VP/cell of Ad-HEX for 1.5 hours on day 6 and cultured for 3 days on a Matrigel (BD) in hESF-DIF (Cell Science & Technology Institute) medium supplemented with the 10 μg/ml human recombinant insulin, 5 μg/ml human apotransferrin, 10 μmol/l 2-mercaptoethanol, 10 μmol/l ethanolamine, 10 μmol/l sodium selenite, 0.5 mg/ml BSA, 20 ng/ml bone morphogenetic protein 4 (R&D Systems), and 20 ng/ml FGF4 (R&D Systems). In hepatic differentiation, hepatoblasts were transduced with 3,000 VP/cell of Ad-LacZ or Ad-HNF4α for 1.5 hr on day 9 and were cultured for 11 days on Matrigel (BD) in L15 medium (Invitrogen, Carlsbad, CA) supplemented with 8.3% tryptose phosphate broth (BD), 8.3% fetal bovine serum (Vita, Chiba, Japan), 10 μmol/l hydrocortisone 21-hemisuccinate (Sigma), 1 μmol/l insulin, 25 mmol/l $NaHCO_3$ (Wako, Osaka, Japan), 20 ng/ml hepatocyte growth factor (R&D Systems), 20 ng/ml Oncostatin M (R&D Systems), and 10^{-6} mol/l Dexamethasone (Sigma).

Ad vectors. Ad vectors were constructed by an improved *in vitro* ligation method.[42,43] The human HNF4α gene (accession number NM_000457) was amplified by PCR using primers designed to incorporate the 5′ Not I and 3′ Xba I restriction enzyme sites: Fwd 5′-ggcctctagatggaggcagggagaatg-3′ and Rev 5′-ccccgcggccgcagcggcttgctagataac-3′. The human HNF4α gene was inserted into pBSKII (Invitrogen), resulting in pBSKII-HNF4α, and then the human HNF4α gene was inserted into pHMEF5,[44] which contains the human elongation factor-1α (EF-1α) promoter, resulting in pHMEF-HNF4α. The pHMEF-HNF4α was digested with I-CeuI/PI-SceI and ligated into I-Ceu I/PI-SceI-digested pAdHM41-K7,[19] resulting in pAd-HNF4α. The human EF-1α promoter-driven LacZ-, SOX17-, or HEX-expressing Ad vectors, Ad-LacZ, Ad-SOX17, or Ad-HEX, were constructed previously.[7,8,45] Ad-LacZ, Ad-SOX17, Ad-HEX, and Ad-HNF4α, each of which contains a stretch of lysine residue (K7) peptides in the C-terminal region of the fiber knob for more efficient transduction of human ESCs, iPSCs, and DE cells, were generated and purified as described previously.[7] The VP titer was determined by using a spectrophotometric method.[46]

LacZ assay. Human ESC- and iPSC-derived cells were transduced with Ad-LacZ at 3,000 VP/cell for 1.5 hours. After culturing for the indicated number of days, 5-bromo-4-chloro-3-indolyl β-D-galactopyranoside (X-Gal) staining was performed as described previously.[44]

Flow cytometry. Single-cell suspensions of human ESCs, iPSCs, and their derivatives were fixed with methanol at 4 °C for 20 minutes and then incubated with the primary antibody, followed by the secondary antibody. Flow cytometry analysis was performed using a FACS LSR Fortessa flow cytometer (BD).

RNA isolation and reverse transcription-PCR. Total RNA was isolated from human ESCs, iPSCs, and their derivatives using ISOGENE (Nippon Gene) according to the manufacturer's instructions. Primary human hepatocytes were purchased from CellzDirect, Durham, NC. complementary DNA was synthesized using 500 ng of total RNA with a Superscript VILO cDNA synthesis kit (Invitrogen). Real-time reverse transcription-PCR was performed with Taqman gene expression assays (Applied Biosystems, Foster City, CA) or SYBR Premix Ex Taq (TaKaRa) using an ABI PRISM 7000 Sequence Detector (Applied Biosystems). Relative quantification was performed against a standard curve and the values were normalized against the input determined for the housekeeping gene, glyceraldehyde 3-phosphate dehydrogenase. The primer sequences used in this study are described in **Supplementary Table S1**.

Immunohistochemistry. The cells were fixed with methanol or 4% paraformaldehyde (Wako). After blocking with phosphate-buffered saline containing 2% BSA (Sigma) and 0.2% Triton X-100 (Sigma), the cells were incubated with primary antibody at 4 °C for 16 hours, followed by incubation with a secondary antibody that was labeled with Alexa Fluor 488 (Invitrogen) or Alexa Fluor 594 (Invitrogen) at room temperature for 1 hour. All the antibodies are listed in **Supplementary Table S2**.

Assay for CYP activity. To measure cytochrome P450 3A4, 2C9, and 1A2 activity, we performed Lytic assays by using a P450-GloTM CYP3A4 Assay Kit (Promega, Madison, WI). For the CYP3A4 and 2C9 activity assay, undifferentiated human ESCs, the hepatocyte-like cells, and primary human hepatocytes were treated with rifampicin (Sigma), which is the substrate for CYP3A4 and CYP2C9, at a final concentration of 25 μmol/l or DMSO (0.1%) for 48 hours. For the CYP1A2 activity assay, undifferentiated human ESCs, the hepatocyte-like cells, and primary human hepatocytes were treated with omeprazole (Sigma), which is the substrate for CYP1A2, at a final concentration of 10 μM or DMSO (0.1%) for 48 hours. We measured the fluorescence activity with a luminometer (Lumat LB 9507; Berthold, Oak Ridge, TN) according to the manufacturer's instructions.

Pyronin Y/Hoechst Staining. Human ESC-derived cells were stained with Hoechst33342 (Sigma) and Pyronin Y (PY) (Sigma) in Dulbecco's modified Eagle medium (Wako) supplemented with 0.2 mmol/l HEPES and 5% FCS (Invitrogen). Samples were then placed on ice for 15 minutes, and 7-AAD was added to a final concentration of 0.5 mg/ml for exclusion of dead cells. Fluorescence-activated cell-sorting analysis of these cells was

performed on a FACS LSR Fortessa flow cytometer (Becton Dickinson) equipped with a UV-laser.

Cellular uptake and excretion of ICG. ICG (Sigma) was dissolved in DMSO at 100 mg/ml, then added to a culture medium of the hepatocyte-like cells to a final concentration of 1 mg/ml on day 20 of differentiation. After incubation at 37 °C for 60 minutes, the medium with ICG was discarded and the cells were washed with phosphate-buffered saline. The cellular uptake of ICG was then examined by microscopy. Phosphate-buffered saline was then replaced by the culture medium and the cells were incubated at 37 °C for 6 hours. The excretion of ICG was examined by microscopy.

Periodic Acid-Schiff assay for glycogen. The hepatocyte-like cells were fixed with 4% paraformaldehyde and stained using a Periodic Acid-Schiff staining system (Sigma) on day 20 of differentiation according to the manufacturer's instructions.

Cell viability tests. Cell viability was assessed by Alamar Blue assay kit (Invitrogen). After treatment with test compounds[47–50] (troglitazone, acetaminophen, cyclophosphamide, and carbamazepine) (all from Wako) for 2 days, the culture medium was replaced with 0.5 mg/ml solution of Alamar Blue in culturing medium and cells were incubated for 3 hours at 37 °C. The supernatants of the cells were measured at a wavelength of 570 nm with background subtraction at 600 nm in a plate reader. Control refers to incubations in the absence of test compounds and was considered as 100% viability value.

Uptake of LDL. The hepatocyte-like cells were cultured with medium containing Alexa-488-labeled LDL (Invitrogen) for 1 hour, and then the cells that could uptake LDL were assessed by immunohistochemistry and flow cytometry.

Primary human hepatocytes. Cryopreserved human hepatocytes were purchased from CellzDirect (lot Hu8072). The vials of hepatocytes were rapidly thawed in a shaking water bath at 37 °C; the contents of the vial were emptied into prewarmed Cryopreserved Hepatocyte Recovery Medium (CellzDirect) and the suspension was centrifuged at 100*g* for 10 minutes at room temperature. The hepatocytes were seeded at 1.25×10^5 cells/cm^2 in hepatocyte culture medium (Lonza, Walkersville, MD) containing 10% FCS (GIBCO-BRL) onto type I collagen-coated 12-well plates. The medium was replaced with hepatocyte culture medium containing 10% FCS (GIBCO-BRL) 6 hours after seeding. The hepatocytes, which were cultured 48 hours after plating the cells, were used in the experiments.

SUPPLEMENTARY MATERIAL

Figure S1. Genome-wide screening of transcription factors involved in hepatic differentiation emphasizes the importance of the transcription factor HNF4α.
Figure S2. Summary of specific markers for DE cells, hepatoblasts, hepatocytes, cholangiocytes, and pancreas cells.
Figure S3. The formation of DE cells, hepatoblasts, hepatocytes, and cholangiocytes from human ESCs.
Figure S4. Overexpression of HNF4α mRNA in hepatoblasts by Ad-HNF4α transduction.
Figure S5. Time course of LacZ expression in hepatoblasts transduced with Ad-LacZ.
Figure S6. The morphology of the hepatocyte-like cells.
Figure S7. Upregulation of the expression levels of conjugating enzymes and hepatic transporters by HNF4α transduction.
Figure S8. Upregulation of the expression levels of hepatic transcription factors by HNF4α transduction.
Figure S9. Generation of hepatocytes from various human ES or iPS cell lines.
Figure S10. Promotion of MET by HNF4α transduction.
Figure S11. Arrest of cell growth by HNF4α transduction.
Table S1. List of Taqman probes and primers used in this study.
Table S2. List of antibodies used in this study.

ACKNOWLEDGMENTS

We thank Hiroko Matsumura and Misae Nishijima for their excellent technical support. H.M., M.K.F., and T.H. were supported by grants from the Ministry of Health, Labor, and Welfare of Japan. H.M. was also supported by Japan Research foundation For Clinical Phamacology, The Nakatomi Foundation, and The Uehara Memorial Foundation. K.K. (K. Kawabata) was supported by grants from the Ministry of Education, Sports, Science and Technology of Japan (20200076) and the Ministry of Health, Labor, and Welfare of Japan. K.K. (K. Katayama) and F.S. was supported by Program for Promotion of Fundamental Studies in Health Sciences of the National Institute of Biomedical Innovation (NIBIO).

REFERENCES

1. Thomson, JA, Itskovitz-Eldor, J, Shapiro, SS, Waknitz, MA, Swiergiel, JJ, Marshall, VS *et al.* (1998). Embryonic stem cell lines derived from human blastocysts. *Science* **282**: 1145–1147.
2. Takahashi, K, Tanabe, K, Ohnuki, M, Narita, M, Ichisaka, T, Tomoda, K *et al.* (2007). Induction of pluripotent stem cells from adult human fibroblasts by defined factors. *Cell* **131**: 861–872.
3. Murry, CE and Keller, G (2008). Differentiation of embryonic stem cells to clinically relevant populations: lessons from embryonic development. *Cell* **132**: 661–680.
4. Basma, H, Soto-Gutiérrez, A, Yannam, GR, Liu, L, Ito, R, Yamamoto, T *et al.* (2009). Differentiation and transplantation of human embryonic stem cell-derived hepatocytes. *Gastroenterology* **136**: 990–999.
5. Touboul, T, Hannan, NR, Corbineau, S, Martinez, A, Martinet, C, Branchereau, S *et al.* (2010). Generation of functional hepatocytes from human embryonic stem cells under chemically defined conditions that recapitulate liver development. *Hepatology* **51**: 1754–1765.
6. Duan, Y, Ma, X, Ma, X, Zou, W, Wang, C, Bahbahan, IS *et al.* (2010). Differentiation and characterization of metabolically functioning hepatocytes from human embryonic stem cells. *Stem Cells* **28**: 674–686.
7. Inamura, M, Kawabata, K, Takayama, K, Tashiro, K, Sakurai, F, Katayama, K *et al.* (2011). Efficient generation of hepatoblasts from human ES cells and iPS cells by transient overexpression of homeobox gene HEX. *Mol Ther* **19**: 400–407.
8. Takayama, K, Inamura, M, Kawabata, K, Tashiro, K, Katayama, K, Sakurai, F *et al.* (2011). Efficient and directive generation of two distinct endoderm lineages from human ESCs and iPSCs by differentiation stage-specific SOX17 transduction. *PLoS ONE* **6**: e21780.
9. Duncan, SA, Manova, K, Chen, WS, Hoodless, P, Weinstein, DC, Bachvarova, RF *et al.* (1994). Expression of transcription factor HNF-4 in the extraembryonic endoderm, gut, and nephrogenic tissue of the developing mouse embryo: HNF-4 is a marker for primary endoderm in the implanting blastocyst. *Proc Natl Acad Sci USA* **91**: 7598–7602.
10. Taraviras, S, Monaghan, AP, Schütz, G and Kelsey, G (1994). Characterization of the mouse HNF-4 gene and its expression during mouse embryogenesis. *Mech Dev* **48**: 67–79.
11. Parviz, F, Matullo, C, Garrison, WD, Savatski, L, Adamson, JW, Ning, G *et al.* (2003). Hepatocyte nuclear factor 4alpha controls the development of a hepatic epithelium and liver morphogenesis. *Nat Genet* **34**: 292–296.
12. Odom, DT, Zizlsperger, N, Gordon, DB, Bell, GW, Rinaldi, NJ, Murray, HL *et al.* (2004). Control of pancreas and liver gene expression by HNF transcription factors. *Science* **303**: 1378–1381.
13. Battle, MA, Konopka, G, Parviz, F, Gaggl, AL, Yang, C, Sladek, FM *et al.* (2006). Hepatocyte nuclear factor 4alpha orchestrates expression of cell adhesion proteins during the epithelial transformation of the developing liver. *Proc Natl Acad Sci USA* **103**: 8419–8424.
14. Konopka, G, Tekiela, J, Iverson, M, Wells, C and Duncan, SA (2007). Junctional adhesion molecule-A is critical for the formation of pseudocanaliculi and modulates E-cadherin expression in hepatic cells. *J Biol Chem* **282**: 28137–28148.
15. Li, J, Ning, G and Duncan, SA (2000). Mammalian hepatocyte differentiation requires the transcription factor HNF-4alpha. *Genes Dev* **14**: 464–474.
16. Hayhurst, GP, Lee, YH, Lambert, G, Ward, JM and Gonzalez, FJ (2001). Hepatocyte nuclear factor 4alpha (nuclear receptor 2A1) is essential for maintenance of hepatic gene expression and lipid homeostasis. *Mol Cell Biol* **21**: 1393–1403.
17. Khurana, S, Jaiswal, AK and Mukhopadhyay, A (2010). Hepatocyte nuclear factor-4alpha induces transdifferentiation of hematopoietic cells into hepatocytes. *J Biol Chem* **285**: 4725–4731.
18. Suetsugu, A, Nagaki, M, Aoki, H, Motohashi, T, Kunisada, T and Moriwaki, H (2008). Differentiation of mouse hepatic progenitor cells induced by hepatocyte nuclear factor-4 and cell transplantation in mice with liver fibrosis. *Transplantation* **86**: 1178–1186.
19. Koizumi, N, Mizuguchi, H, Utoguchi, N, Watanabe, Y and Hayakawa, T (2003). Generation of fiber-modified adenovirus vectors containing heterologous peptides in both the HI loop and C terminus of the fiber knob. *J Gene Med* **5**: 267–276.
20. Shiojiri, N (1984). The origin of intrahepatic bile duct cells in the mouse. *J Embryol Exp Morphol* **79**: 25–39.
21. Moll, R, Franke, WW, Schiller, DL, Geiger, B and Krepler, R (1982). The catalog of human cytokeratins: patterns of expression in normal epithelia, tumors and cultured cells. *Cell* **31**: 11–24.

22. Antoniou, A, Raynaud, P, Cordi, S, Zong, Y, Tronche, F, Stanger, BZ *et al.* (2009). Intrahepatic bile ducts develop according to a new mode of tubulogenesis regulated by the transcription factor SOX9. *Gastroenterology* **136**: 2325–2333.
23. Offield, MF, Jetton, TL, Labosky, PA, Ray, M, Stein, RW, Magnuson, MA *et al.* (1996). PDX-1 is required for pancreatic outgrowth and differentiation of the rostral duodenum. *Development* **122**: 983–995.
24. Sussel, L, Kalamaras, J, Hartigan-O'Connor, DJ, Meneses, JJ, Pedersen, RA, Rubenstein, JL *et al.* (1998). Mice lacking the homeodomain transcription factor Nkx2.2 have diabetes due to arrested differentiation of pancreatic beta cells. *Development* **125**: 2213–2221.
25. Ingelman-Sundberg, M, Oscarson, M and McLellan, RA (1999). Polymorphic human cytochrome P450 enzymes: an opportunity for individualized drug treatment. *Trends Pharmacol Sci* **20**: 342–349.
26. Henderson, CJ, Otto, DM, Carrie, D, Magnuson, MA, McLaren, AW, Rosewell, I *et al.* (2003). Inactivation of the hepatic cytochrome P450 system by conditional deletion of hepatic cytochrome P450 reductase. *J Biol Chem* **278**: 13480–13486.
27. Yamada, T, Yoshikawa, M, Kanda, S, Kato, Y, Nakajima, Y, Ishizaka, S *et al.* (2002). *In vitro* differentiation of embryonic stem cells into hepatocyte-like cells identified by cellular uptake of indocyanine green. *Stem Cells* **20**: 146–154.
28. Anzenbacher, P and Anzenbacherová, E (2001). Cytochromes P450 and metabolism of xenobiotics. *Cell Mol Life Sci* **58**: 737–747.
29. Zhao, D, Chen, S, Cai, J, Guo, Y, Song, Z, Che, J *et al.* (2009). Derivation and characterization of hepatic progenitor cells from human embryonic stem cells. *PLoS ONE* **4**: e6468.
30. Hatta, K, Takagi, S, Fujisawa, H and Takeichi, M (1987). Spatial and temporal expression pattern of N-cadherin cell adhesion molecules correlated with morphogenetic processes of chicken embryos. *Dev Biol* **120**: 215–227.
31. Shiojiri, N (1981). Enzymo- and immunocytochemical analyses of the differentiation of liver cells in the prenatal mouse. *J Embryol Exp Morphol* **62**: 139–152.
32. Lee, JM, Dedhar, S, Kalluri, R and Thompson, EW (2006). The epithelial-mesenchymal transition: new insights in signaling, development, and disease. *J Cell Biol* **172**: 973–981.
33. Macleod, KF, Sherry, N, Hannon, G, Beach, D, Tokino, T, Kinzler, K *et al.* (1995). p53-dependent and independent expression of p21 during cell growth, differentiation, and DNA damage. *Genes Dev* **9**: 935–944.
34. Si-Tayeb, K, Noto, FK, Nagaoka, M, Li, J, Battle, MA, Duris, C *et al.* (2010). Highly efficient generation of human hepatocyte-like cells from induced pluripotent stem cells. *Hepatology* **51**: 297–305.
35. Sekiya, S and Suzuki, A (2011). Direct conversion of mouse fibroblasts to hepatocyte-like cells by defined factors. *Nature* **475**: 390–393.
36. Huang, P, He, Z, Ji, S, Sun, H, Xiang, D, Liu, C *et al.* (2011). Induction of functional hepatocyte-like cells from mouse fibroblasts by defined factors. *Nature* **475**: 386–389.
37. Satohisa, S, Chiba, H, Osanai, M, Ohno, S, Kojima, T, Saito, T *et al.* (2005). Behavior of tight-junction, adherens-junction and cell polarity proteins during HNF-4alpha-induced epithelial polarization. *Exp Cell Res* **310**: 66–78.
38. Xu, ZL, Mizuguchi, H, Sakurai, F, Koizumi, N, Hosono, T, Kawabata, K *et al.* (2005). Approaches to improving the kinetics of adenovirus-delivered genes and gene products. *Adv Drug Deliv Rev* **57**: 781–802.
39. Nagata, S, Toyoda, M, Yamaguchi, S, Hirano, K, Makino, H, Nishino, K *et al.* (2009). Efficient reprogramming of human and mouse primary extra-embryonic cells to pluripotent stem cells. *Genes Cells* **14**: 1395–1404.
40. Makino, H, Toyoda, M, Matsumoto, K, Saito, H, Nishino, K, Fukawatase, Y *et al.* (2009). Mesenchymal to embryonic incomplete transition of human cells by chimeric OCT4/3 (POU5F1) with physiological co-activator EWS. *Exp Cell Res* **315**: 2727–2740.
41. Furue, MK, Na, J, Jackson, JP, Okamoto, T, Jones, M, Baker, D *et al.* (2008). Heparin promotes the growth of human embryonic stem cells in a defined serum-free medium. *Proc Natl Acad Sci USA* **105**: 13409–13414.
42. Mizuguchi, H and Kay, MA (1998). Efficient construction of a recombinant adenovirus vector by an improved *in vitro* ligation method. *Hum Gene Ther* **9**: 2577–2583.
43. Mizuguchi, H and Kay, MA (1999). A simple method for constructing E1- and E1/E4-deleted recombinant adenoviral vectors. *Hum Gene Ther* **10**: 2013–2017.
44. Kawabata, K, Sakurai, F, Yamaguchi, T, Hayakawa, T and Mizuguchi, H (2005). Efficient gene transfer into mouse embryonic stem cells with adenovirus vectors. *Mol Ther* **12**: 547–554.
45. Tashiro, K, Kawabata, K, Sakurai, H, Kurachi, S, Sakurai, F, Yamanishi, K *et al.* (2008). Efficient adenovirus vector-mediated PPAR gamma gene transfer into mouse embryoid bodies promotes adipocyte differentiation. *J Gene Med* **10**: 498–507.
46. Maizel, JV Jr, White, DO and Scharff, MD (1968). The polypeptides of adenovirus. I. Evidence for multiple protein components in the virion and a comparison of types 2, 7A, and 12. *Virology* **36**: 115–125.
47. Smith, MT (2003). Mechanisms of troglitazone hepatotoxicity. *Chem Res Toxicol* **16**: 679–687.
48. Dai, Y and Cederbaum, AI (1995). Cytotoxicity of acetaminophen in human cytochrome P4502E1-transfected HepG2 cells. *J Pharmacol Exp Ther* **273**: 1497–1505.
49. Chang, TK, Weber, GF, Crespi, CL and Waxman, DJ (1993). Differential activation of cyclophosphamide and ifosphamide by cytochromes P-450 2B and 3A in human liver microsomes. *Cancer Res* **53**: 5629–5637.
50. Miao, XS and Metcalfe, CD (2003). Determination of carbamazepine and its metabolites in aqueous samples using liquid chromatography-electrospray tandem mass spectrometry. *Anal Chem* **75**: 3731–3738.

Journal of Chromatography B, 879 (2011) 2928–2934

Contents lists available at SciVerse ScienceDirect

Journal of Chromatography B

journal homepage: www.elsevier.com/locate/chromb

Rapid and sensitive analyses of glycoprotein-derived oligosaccharides by liquid chromatography and laser-induced fluorometric detection capillary electrophoresis

Takehiro Oyama, Masahiro Yodohsi, Ayako Yamane, Kazuaki Kakehi, Takao Hayakawa, Shigeo Suzuki*

Faculty of Pharmaceutical Sciences, Kinki University, Japan

ARTICLE INFO

Article history:
Received 30 April 2011
Accepted 21 August 2011
Available online 26 August 2011

Keywords:
Glycoprotein
N-linked oligosaccharides
High-performance liquid chromatography
Capillary electrophoresis with
laser-induced fluorometric detection

ABSTRACT

Asparagine-type oligosaccharides are released from core proteins as *N*-glycosylamines in the initial step of the action of the peptide N^4-(*N*-acetyl-β-D-glucosaminyl)asparagine amidase F (PNGase F). The released *N*-glycosylamine-type oligosaccharides (which are exclusively present at least during the course of the enzyme reaction) could therefore be derivatized with amine-labeling reagents. Here we report a method using 4-fluoro-7-nitro-2,1,3-benzoxadiazole (NBD-F) as a labeling reagent for glycosylamine-type oligosaccharides. We applied the method for the sensitive analysis of some oligosaccharide mixtures derived from well-characterized glycoproteins including human transferrin, α_1-acid glycoprotein, bovine fetuin, and ribonuclease B. NBD-labeled oligosaccharides were successfully separated on an amide-bonded column or a diol-silica column. This labeling method included the release of oligosaccharides from glycoproteins and derivatization of oligosaccharides in a one-pot reaction and was completed within 3 h. The method showed approximately fivefold higher sensitivity than that involving labeling with ethyl *p*-aminobenzoate (ABEE) in HPLC using fluorometric detection and a one order of magnitude higher response in ESI-LC/MS. We also applied this method for the sensitive analysis of glycoprotein-derived oligosaccharides by capillary electrophoresis with laser-induced fluorometric detection (LIF-CE). The limit of detection in HPLC and LIF-CE were 100 fmol and 4 fmol, respectively.

1. Introduction

The most abundant post-translational modification of proteins in nature is glycosylation. Understanding the function of glycans and their changes in relation to diseases has been complicated by challenges associated with their characterization. Particular carbohydrate sequences and linkages at each glycosylation site can vary considerably and contribute to heterogeneity. Their comprehensive characterization is only possible by high-resolution separation techniques following to sensitive fluorescent labeling. Several labeling methods with fluorogenic reagents have been developed for the analysis of asparagine-type oligosaccharides [1]. The methods using 2-aminopyridine (AP) [2] and ethyl *p*-aminobenzoate (ABEE) [3] are widely used for high-performance liquid chromatography (HPLC) with fluorometric detection. Takahashi and colleagues prepared ~600 AP-labeled asparagine-type oligosaccharides and completed three-dimensional mapping of their elution indices obtained on octadecyl-bonded silica (ODS)-, amide- and diethylaminoethyl (DEAE)-bonded columns [4–6]. The retention indices are available at the website [7]. 8-Aminopyrene-1,3,6-trisulfonate (APTS) is an important labeling reagent for high-resolution analyses of oligosaccharides by capillary electrophoresis (CE) because three sulfonate groups generate high mobility [8–11]. Moreover, the excitation maxima of APTS derivatives shift hyperchromically from 420 nm to 456 nm, which enables specific detection of the derivatives via laser-induced fluorometric-capillary electrophoresis (LIF-CE) using an argon laser (488 nm) as the light source [12]. We also reported 7-amino-4-methylcoumarin to be a sensitive labeling reagent for oligosaccharides, and applied fluorescence-detection HPLC of some oligosaccharides derived from glycoproteins [13]. These labeling methods are based on a common reaction scheme called "reductive amination". This requires two-step reactions (*i.e.*, Schiff base formation and reduction of the Schiff base to corresponding 1-aminoalditol derivatives), and usually involves tedious purification steps of the labeled oligosaccharides. These derivatization reactions must be carried out under acidic conditions, which are often conducted at relatively

Abbreviations: ABEE, ethyl *p*-aminobenzoate; AP, 2-aminopyridine; APTS, 8-aminopyrene-1,3,6-trisulfonate; Fmoc-Cl, 9-fluorenylmethyl chloroformate; PNGase F, peptide N^4-(*N*-acetyl-β-D-glucosaminyl)asparagine amidase F; CE, capillary electrophoresis; LIF, laser-induced fluorometric detection.

* Corresponding author at: Department of Pharmacy, Faculty of Pharmaceutical Sciences, Kinki University, 3-4-1 Kowakae, Higashi-osaka, Osaka 577-8502, Japan. Tel.: +81 6 6721 2332; fax: +81 6 6721 2353.
E-mail address: suzuki@phar.kindai.ac.jp (S. Suzuki).

1570-0232/$ – see front matter © 2011 Elsevier B.V. All rights reserved.
doi:10.1016/j.jchromb.2011.08.026

low temperatures for a long time to avoid hydrolysis of the sialic acid residues.

We reported another type of fluorescent derivatization of *N*-linked oligosaccharides as released from glycoproteins using 9-fluorenylmethyl chloroformate (Fmoc-Cl), which is based on the labeling of glycosylamines generated by the action of PNGase F [14]. In general, *N*-glycosylamine-type oligosaccharides released by the action of PNGase F are chemically stable, and are exclusively present at least during the course of the enzyme reaction. However, they are subjected to hydrolysis to form free oligosaccharides by overnight incubation or treatment with acid. The glycosylamine-type oligosaccharides in the digestion mixture can be derivatized with Fmoc-Cl. Fmoc labeling has three main advantages. Firstly, Fmoc derivatives of glycosylamines have a single configuration (*i.e.* β-form) at the reducing end, and have no isomers that complicate the chromatograms. Second, Fmoc residues have strong fluorescence at 310 nm by irradiation at 266 nm. Thirdly, the Fmoc group is readily removed by incubation with morpholine in dimethylformamide at mild conditions. The main disadvantage is that Fmoc derivatives fluoresce with low wavelength light (266 nm), which often coincides with the faint fluorescence of contaminants in the reaction mixture.

Here we report a method using NBD-F as a fluorometric reagent for labeling glycosylamine-type oligosaccharides. We applied the method for sensitive detection of glycoprotein-derived oligosaccharides in HPLC and CE with LIF detection. NBD-labeled oligosaccharides were successfully analyzed on normal-phase, chemically bonded silica columns. The described method showed approximately fivefold higher sensitivities than oligosaccharides labeled with ABEE or Fmoc-Cl. We also applied LIF-CE for the analysis of NBD-labeled oligosaccharides. Sensitivity was high and the detection limits were at the fmol level.

2. Experimental

2.1. Materials

Peptide-N^4-(*N*-acetyl-β-D-glucosaminyl)asparagine amidase (PNGase F; EC 3.5.1.52, recombinant) was obtained from Roche Diagnostics (Mannheim, Germany). 4-Fluoro-7-nitro-2,1,3-benzoxadiazole (NBD-F) and ethyl *p*-aminobenzoate (ABEE) were obtained from Tokyo Kasei (Chuo-ku, Tokyo, Japan). α_1-Acid glycoprotein (human), transferrin (human), ribonuclease B (bovine pancreas), and sodium cyanoborohydride were obtained from Sigma–Aldrich Japan (Shinagawa-ku, Tokyo, Japan). Fetuin (bovine) was obtained from Gibco (Invitrogen, Chuo-ku, Tokyo, Japan). Ovalbumin was purified from chicken eggs according to the method reported by Kekwick and Cannan [15]. Other reagents and solvents used in the present study were reagent grade or HPLC grade, and purchased from Wako (Dosho-machi, Chuo-ku, Osaka, Japan).

2.2. Release of N-Linked oligosaccharides and NBD derivatization

Release of *N*-linked oligosaccharides from a glycoprotein sample followed by labeling with NBD-F was undertaken in a one-pot reaction. Briefly, a sample of glycoprotein (100 μg) dissolved in 10 μL 20 mM phosphate buffer (pH 8.0), and solution heated at 100 °C for 5 min. After cooling, 1 μL of PNGase F (0.2 unit) was added to the mixture, and incubated at 37 °C for 2 h. After the mixture was heated on a boiling water-bath for 2 min, a freshly prepared solution of 0.3 M NBD-F in acetonitrile (5 μL) was added, and the mixture heated at 70 °C for 5 min. Water (100 μL) and dichloromethane (200 μL) were added to the mixture. The solution was shaken vigorously and the dichloromethane layer carefully removed. The same procedure for extraction with dichloromethane was repeated twice. Finally, the aqueous layer containing NBD-labeled glycosylamine-type oligosaccharides was evaporated to dryness by a centrifugal evaporator (Tomy, CC-101). The residue was dissolved in 100 μL of water and a portion (typically 5 μL) was used for the analysis by HPLC and CE. Dried samples were stable for at least several months at −20 °C.

2.3. Derivatization of glycoprotein-derived oligosaccharides with Fmoc-Cl and ABEE

Derivatization of the released glycosylamine-type oligosaccharides with Fmoc-Cl has been described [14]. ABEE derivatization and purification of the labeled oligosaccharides were carried out according to the method of Wang et al. [3]. Briefly, PNGase F digests of a glycoprotein (100 μg) were mixed with 1 μL of acetic acid. The reaction mixture was dried and dissolved in each 20 μL aliquot of the freshly prepared solution of ABEE (165 mg or 1 mmol) dissolved in 1 mL of a mixture of acetic acid–methanol (41:250, v/v) and sodium cyanoborohydride (35 mg) in methanol (1 mL). The reaction mixture was kept at 80 °C for 60 min. After cooling, the solution was dissolved in 100 μL of water. Excess ABEE was removed by extraction twice with each 200 μL aliquot of ethyl acetate. The aqueous phase obtained was evaporated to dryness using a centrifugal evaporator. The residue was dissolved in 100 μL of water and a portion (5 μL) used for the analysis by HPLC.

2.4. HPLC analyses

For HPLC analyses we used a Prominence system (Shimadzu, Nakagyo-ku, Kyoto, Japan). This consisted of a UFLC LC-20AD pump, a SIL-20AC auto sampler, a DGU-20A3 degasser, a CTO-20A column oven, and a RF10AXL fluorescence detector controlled with a LCMSstation® system. NBD-, Fmoc- and ABEE-labeled oligosaccharides derived from transferrin were separated on an Amide80 column (Tosoh, Tokyo, Japan; 4.6 mm i.d., 250 mm) thermostated at 40 °C using a linear gradient formed by 0.1% (v/v) acetic acid in acetonitrile (solvent A) and an aqueous solution of 0.2% acetic acid/3% triethylamine (solvent B) at a flow rate of 1.0 mL/min. The column was initially equilibrated and eluted with 23% solvent B for 5 min. Then a mixing ratio of solvent B was increased linearly to 44% over 75 min and then further increased to 95% over 10 min. The column was equilibrated under initial conditions for 15 min before the next injection. NBD-labeled acidic oligosaccharides from glycoproteins were separated under identical conditions except for the gradient program: 20–25% B for 5 min, 25–35% B from 5 to 80 min, and 35–95% B from 80 to 90 min. NBD derivatives of neutral oligosaccharides from glycoproteins were separated on an Inertsil diol column (GL Science, Tokyo, Japan; 4.6 mm i.d., 250 mm) at a flow rate of 1.0 mL/min with a linear gradient using 0.1% trifluoroacetic acid (TFA; solvent A) and 95% acetonitrile containing 0.1% TFA (solvent B); 99% solvent B for 5 min, 99–75% solvent B from 5 to 15 min, 75–50% from 15 to 75 min, and 50% to 1% solvent B from 75 to 80 min. Fluorometric detection was undertaken at 470 nm (excitation)/540 nm (emission) for NBD derivatives, 266 nm (excitation)/310 nm (emission) for Fmoc derivatives, 310 nm (excitation)/370 nm (emission) for ABEE derivatives.

The LC–MS system comprised a quadrupole-ion-trap and time-of-flight mass spectrometer (LC-QIT-TOF-MS; Shimadzu). The detection conditions were: probe voltage, 4.5 kV; detector voltage, −1.7 kV; capillary temperature, 200 °C; flow rate of nebulizer gas, 1.5 L/min; mass range, *m/z* 1200–2400 for neutral saccharides and *m/z* 800–2000 for acidic saccharides; ion trapping time, 30 ms; and scan rate, 5 s/scan. A mixture of ABEE-labeled glucose oligomers was used for the calibration of molecular masses.

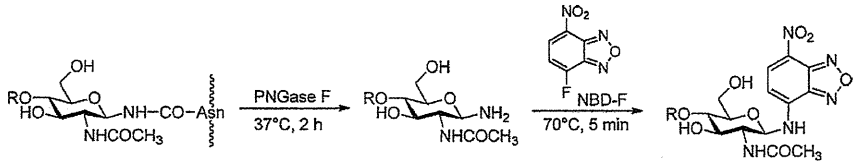

Scheme 1. Enzymatic release of glycosylamine-type oligosaccharides by the action of PNGase F and their derivatization with 4-fluoro-7-nitrobenzofurazan (NBD-F).

2.5. Capillary electrophoresis of NBD-labeled oligosaccharides

Beckman Coulter P/ACE MDQ equipped with an argon ion laser GLA3050A (Showa Optronics, Tokyo, Japan) was used with 32Karat (ver. 8.0) software for data processing and system controlling (Beckman Coulter, Brea, CA, USA). A polydimethylsiloxane-coated capillary, Inert Cap I® (50 μm i.d.; 50 cm in total and 40 cm for effective length; GL Sciences) was used. A detection system setup for fluorescein (488 nm (excitation)/522 nm (emission)). The capillary was washed with water (20 psi, 2 min), and then filled with 100 mM borate buffer (pH 8.3) containing 5% polyethylene glycol 2000 (20 psi, 0.5 min). A NBD-labeled sample was injected at 1 psi for 10 s, and separated by applying the voltage at −15 kV.

3. Results and discussion

3.1. Reaction scheme

PNGase F has been used for releasing asparagine-linked oligosaccharides from glycoproteins. If a glycoprotein containing asparagine-linked oligosaccharides is incubated with PNGase F, the amide linkage between an oligosaccharide and asparagine in a peptide sequence is hydrolyzed to form β-glycosylamine oligosaccharide and aspartic acid [16]. β-Glycosylamine-type oligosaccharides are gradually converted to free oligosaccharides. The stability of the glycosylamine is sensitive to the pH of the reaction solution. Glycosylamine oligosaccharides are stable at weak alkaline media (pH ≈ 8.0), and the rate of hydrolysis from the glycosylamine to free oligosaccharide is very slow [17]. We previously reported the conversion of glycosylamines to the corresponding Fmoc derivatives by an *in situ* derivatization reaction. Here we propose NBD-F as an alternative reagent for labeling glycosylamines because the reaction of amines with this reagent proceeds under the slightly basic conditions. Moreover NBD-labeled glycosylamine fluoresces at 480 nm or irradiating with an argon laser beam which is frequently used for as a light source for fluorimetric detection. We re-examined the reaction conditions and applied them to oligosaccharides of various glycoprotein specimens. The overall reaction scheme is depicted in Scheme 1.

3.2. Optimization studies for the labeling of glycosylamine oligosaccharides released from glycoprotein samples

The NBD derivatization method was optimized by using human serum transferrin as a model glycoprotein. This glycoprotein contains biantennary oligosaccharides with two sialic acids as a main oligosaccharide (approximately >85%) [18]. As described above, glycosylamines derived from glycoproteins are stable in weak alkaline media. Labeling of amines with NBD-F also preferentially proceeds in alkaline media. Therefore, we optimized reaction conditions by changing the concentration and pH of alkaline phosphate buffer for the glycosylamine-releasing reaction with PNGase F followed by NBD labeling.

Recovery of NBD-oligosaccharides was evaluated by the peak area of the main oligosaccharide of transferrin obtained by HPLC analyses (Fig. 1). The buffer pH was optimal at 8.0. The concentration of buffer was not so critical but seemed to be optimal at 20–100 mM. Under optimized conditions using 20 mM phosphate (pH 8.0), the reaction rate of NBD labeling was enhanced with reagent concentration, and almost reached a plateau at 300 mM NBD-F solution. Slight decrease of the products at higher buffer concentration at high temperature indicates the decomposition of

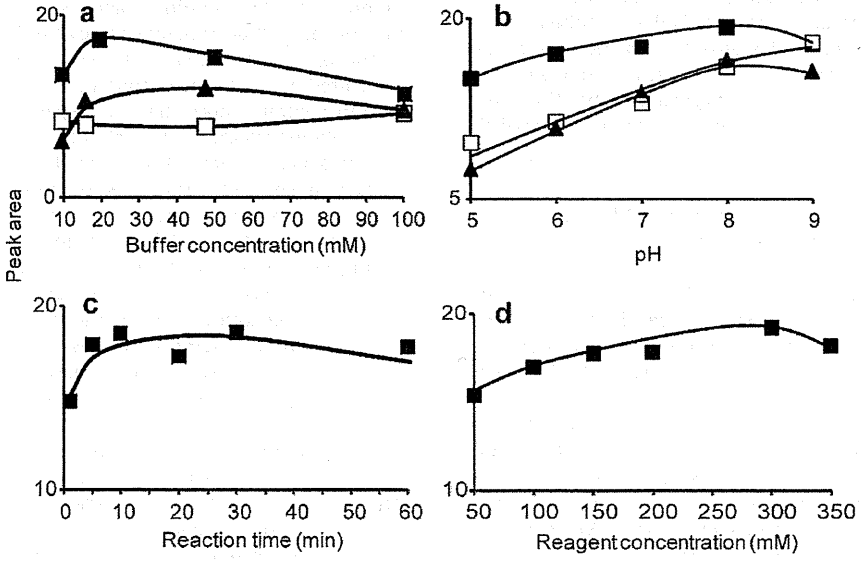

Fig. 1. Effects of buffer concentration (a), pH (b), reaction time (c), and reagent concentration (d) on NBD derivatization of a biantennary oligosaccharide at 70 °C. Unless otherwise depicted in plots, transferrin-derived oligosaccharides (5 μg as a glycoprotein) in each buffer (pH 8.0, 20 μL) were mixed with an acetonitrile solution of NBD-F (300 mM, 5 μL), and the mixture incubated at 70 °C for 10 min. (■) Sodium phosphate, (□) sodium borate, and (▲) ammonium phosphate.

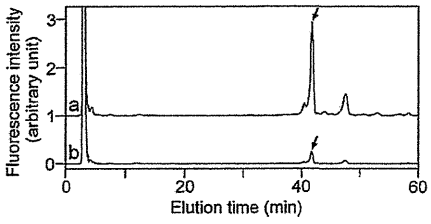

Fig. 2. HPLC analyses of free oligosaccharides as ABEE derivatives as remaining in a reaction mixture after NBD labeling (b) with reference (a). Analytical condition: column; Amide80 (4.6 mm i.d. × 250 mm), eluent; (A) acetonitrile containing 0.1% acetic acid, and (B) 0.2% acetic acid containing 0.2% triethylamine, gradient program; 20% (B) for 5 min, 20–40% (B) for 75 min, 40–95% (B) for 10 min, flow rate; 1.0 mL/min, fluorometric detection; 310 nm (excitation)/370 nm (emission), amount of injection; 5 μg as a glycoprotein.

the NBD derivatives [19]. The NBD labeling seemed to be completed within 5 min at 70 °C using 300 mM NBD-F. A 2 h reaction of PNGase F in 20 mM phosphate buffer (pH 8.0) for the generation of oligosaccharide glycosylamines and labeling by adding 300 mM NBD-F and heating at 70 °C for 5 min was chosen as the optimal conditions for derivatization. The repeatability of this method is also assayed based on the peak area of samples independently prepared from 50 μg of transferrin. We found 4.1% ($n = 5$) as RSD.

For the next experiment, we estimated the amount of unlabeled oligosaccharides remaining in the reaction mixture. The reaction mixture of PNGase F digestion was divided into two equal portions. To one portion was added acetic acid to form free oligosaccharides; it was then labeled with ABEE under standard conditions. The other portion was converted to NBD-labeled glycosylamine-type oligosaccharides as described above. The reaction mixture was further derivatized with ABEE. We estimated the proportion of NBD-unlabeled oligosaccharides from comparison of these two peak intensities of ABEE-labeled oligosaccharides obtained by HPLC (Fig. 2). ABEE derivatives of major biantennary oligosaccharides of transferrin appeared at 42 min. Compared with the upper trace of the direct derivatization mixture, ABEE derivatives after PNGase F digestion/NBD-F labeling were 9.2% of that for the upper trace. That is, >90% of oligosaccharides were released as glycosylamine and labeled with NBD-F. We believe that 9.2% of transferrin glycans are converted to free oligosaccharides in the process of PNGase F digestion because derivatization with NBD-F is sufficiently fast. Bynum et al. recently reported that an online reaction system using solid-phase reactors that immobilize PNGase F produces quantitative amounts of glycosylamine-type oligosaccharides [20]. That is, optimizing PNGase F digestion may enhance the recovery of NBD-labeled oligosaccharides in our method.

3.3. Comparison of the detection sensitivities of NBD-labeled oligosaccharides with those of Fmoc-Cl and ABEE

The sensitivity of detection of NBD-labeled glycosylamine-type oligosaccharides was compared with the sensitivity of detection obtained by previously reported PNGase F/Fmoc-Cl derivatives and the reductively aminated derivatives with ABEE. Glycosylamine oligosaccharides from transferrin by PNGase F digestion were divided into three equal portions and derivatized with NBD-F, Fmoc-Cl and ABEE. The resultant chromatograms obtained on an Amide80 column are shown in Fig. 3. The main peak corresponding to a disialylated biantennary oligosaccharide was detected at 28 min, 27 min, and 42 min for NBD-, Fmoc- and ABEE derivatives, respectively. NBD derivatives had the most intense signal. The peak area of NBD derivatives was 4.4 times more intense than that for Fmoc derivatives, and 5.7 times more intense than that for ABEE derivatives.

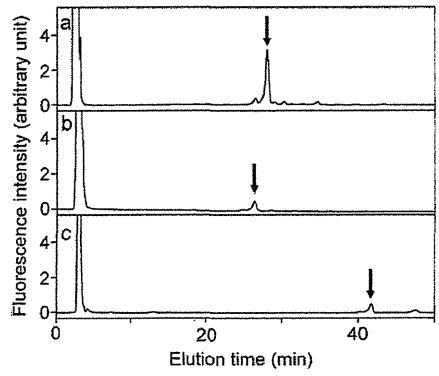

Fig. 3. Comparison of the sensitivity of NBD-labeled (a), Fmoc-labeled (b) and ABEE-labeled (c) oligosaccharides derived from human transferrin. Analytical conditions were identical as those for Fig. 2. Fluorometric detection; (a) 470 nm (excitation)/540 nm (emission), (b) 266 nm (excitation)/310 nm (emission), (c) 310 nm (excitation)/370 nm (emission), amount of injection; 5 μg as a glycoprotein.

3.4. HPLC analyses of oligosaccharides derived from glycoproteins

This PNGase F/NBD labeling method was applied to the HPLC analysis of oligosaccharide mixtures derived from various glycoproteins. We carefully checked the separation conditions, and found an Amide80 column produced good resolution of acidic oligosaccharides.

Fig. 4(a) shows the separation of NBD derivatives of *N*-linked oligosaccharides of human transferrin. To confirm the structures of some oligosaccharides, the derivatives were analyzed by liquid chromatography–electron spray ionization–mass spectrometry (LC–ESI-MS). Peak 1 clearly showed a pseudomolecular ion at m/z 1192 of $[M-2H]^{2-}$ corresponding to a disialylated biantennary oligosaccharide at 28 min as the major peak. Peak 2 showed a molecular ion at m/z 1265 corresponding to a fucosylated disialobiantennary oligosaccharide. Peak 3 at m/z 1046 corresponded to a monosialylated biantennary oligosaccharide.

The method was also applied to the analysis of bovine serum fetuin. Oligosaccharides of this glycoprotein mainly comprise a series of triantennary oligosaccharides containing linkage isomers in one of the lactosamine branches with 2–4 residues of α-2,3- or α-2.6-linked *N*-acetylneuraminic acid [21–23]. Fig. 4(b) shows the result of separation. Large peaks (7 and 8) observed at ~30 min indicated m/z 1520 corresponding to trisialylated oligosaccharides. Fetuin contains more than four species of trisialylated triantennary oligosaccharides. The results indicated that the resolution of Amide80 was not sufficient for the complete resolution of the linkage isomers of trisialylated oligosaccharides. Peak 4 and peak 6 (data not shown) showed the same molecular ions, m/z 1192, corresponding to disialylated oligosaccharides. Peak 5 indicated tetrasialylated oligosaccharides (m/z 1666).

α_1-Acid glycoprotein (AGP; human) has bi-, tri-, and tetraantennary oligosaccharides. Some of the oligosaccharides are fucosylated at the terminal lactosamine residues to form a sialyl Lewis^X structure [24,25]. AGP oligosaccharides were separated based on their molecular size (Fig. 4(c)). Disialobiantennary oligosaccharides (peak 9, m/z 1192) were observed at 28 min as a large peak. Trisialotriantennary oligosaccharides (peaks 10 and 11, m/z 1520) appeared at 29 min and 31 min, respectively, and monofucosylated trisialotriantennary oligosaccharides (peak 12, m/z 1593) appeared at 32 min. Small peaks observed at 33 min to 35 min indicated a series of tetrasialotetraantennary oligosaccharides (peak 13, m/z 1848) and monofucosylated tetrasialotetraantennary oligosaccharides (peak 14, m/z 1921). The complex distribution of the same molecular ion signals may be due to the linkage isomers of *N*-acetyl

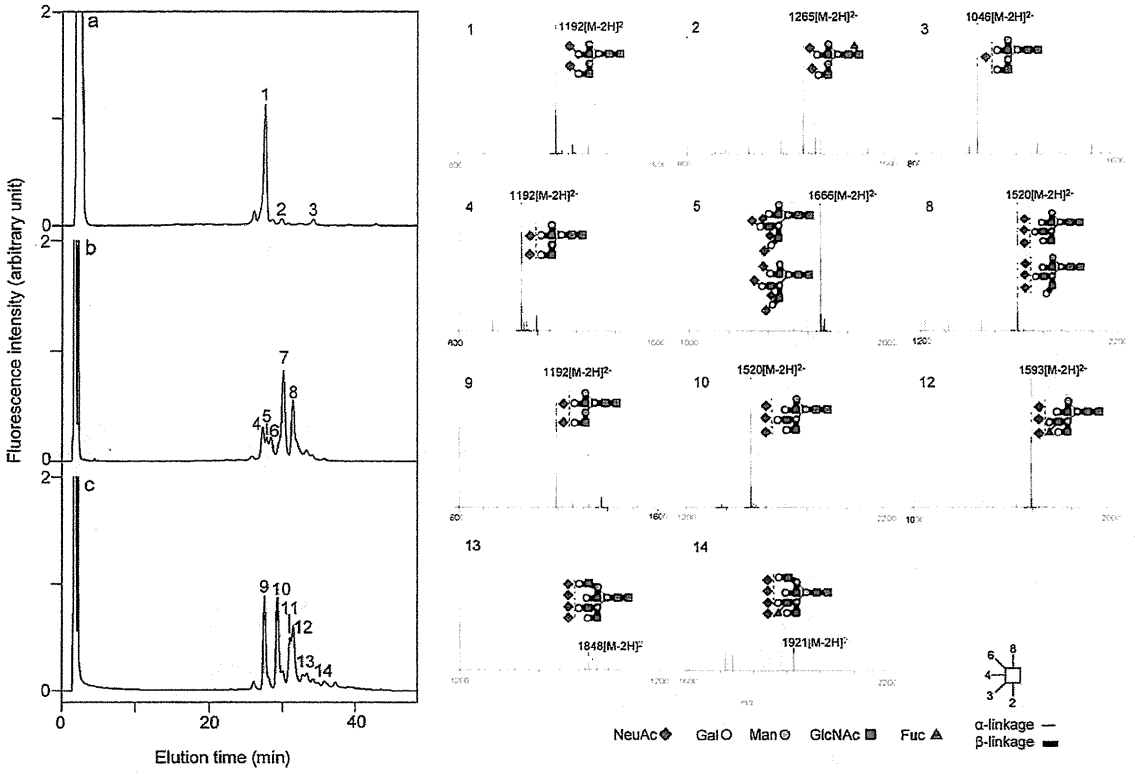

Fig. 4. Application of the PNGase F/NBD method for the HPLC analysis using fluorometric detection of oligosaccharides from human serum transferrin (a), fetal calf serum fetuin (b) and human α_1-acid glycoprotein (c) with ESI-MS spectra of each peak. All MS signals of oligosaccharides with *m/z* values were obtained as the adduct ion of trifluoroacetic acid ($[M+CF_3CO_2]^-$). Analytical conditions: column; Amide80 (4.6 mm i.d. × 250 mm), eluent; (A) acetonitrile containing 0.1% acetic acid (B) 0.2% acetic acid containing 0.2% triethylamine, gradient program; 20–25% (B) for 5 min, 25–35% (B) for 75 min, 35–95% (B) for 10 min, flow rate; 0.8 mL/min, fluorometric detection; 470 nm (excitation)/540 nm (emission), amount of injection; 5 μg as a glycoprotein.

neuraminic acid (NeuAc) residues. NBD derivatization produced pseudomolecular ions of oligosaccharides containing sialic acid at high sensitivity. This may be an advantage for sensitive analyses of minute amounts of carbohydrates in glycoprotein samples.

The described method was also applied to the analysis of carbohydrate chains derived from glycoprotein samples containing neutral oligosaccharides (Fig. 5). We employed a diol column instead of an amide column for the separation of neutral oligosaccharides. This separation mode seemed to be useful for the analysis of complex-type asialooligosacchardies and high mannose-type oligosaccharides.

Ribonuclease B (bovine pancreas) has been reported to contain a series of high mannose-type oligosaccharides, including $Man_{5-9}GlcNAc_2$ [26]. Use of the diol column led to five peaks for these oligosaccharides. In contrast to previously described acidic oligosaccharides, NBD derivatives of a series of high mannose-type oligosaccharides were detected as adduct ions with TFA, $[M+CF_3CO_2]^-$. From the peak identification based on their molecular mass, ribonuclease B oligosaccharides were separated according to molecular size. Moreover, small shoulder peaks observed at the front of peak 3 indicated the presence of linkage isomers of $Man_7GlcNAc_2$ in the terminal α-1,2-linked mannose.

Ovalbumin contains a series of high mannose-type oligosaccharides and bisected hybrid-type oligosaccharides [27–29]. Separation of these oligosaccharides is shown in Fig. 5(b). Peak identification based on the molecular mass of peaks indicated the elution order of the oligosaccharides to be $Man_5GlcNAc_2 < Man_3GlcNAc_5$, $Man_4GlcNAc_4 < Man_6GlcNAc_2$, $Man_4GlcNAc_4 < Man_5GlcNAc_4 < Man_5GlcNAc_6$, $Man_4Gal_1GlcNAc_5$ and/or $Man_5GlcNAc_5$ and $Man_7GlcNAc_2$.

All the data shown above were obtained by injection of 5 μg glycoproteins. Therefore, for example, monofucosylated biantennary oligosaccharides of transferrin occupying ~2% in total of oligosaccharides indicate ~2.5 pmol as the injection amount. Therefore, the lower limit of detection (signal-to-noise (S/N) ratio = 5) in HPLC using fluorometric detection for these oligosaccharides was estimated to be 100 fmol. The sensitivities of NBD-labeled oligosaccharides were compared with those of Fmoc- and ABEE-labeled oligosaccharides in negative ESI-MS analyses: they were 12 times and 10 times higher than those for Fmoc and ABEE derivatives, respectively. The enhanced sensitivity of NBD derivatives indicated the usefulness of this method. However, the resolution of NBD derivatives of oligosaccharides in HPLC was not enough. We therefore applied LIF-CE to the analysis of NBD-labeled glycosylamine-type oligosaccharides.

3.5. Application to CE with LIF detection

LIF-CE was applied to the analysis of NBD-labeled glycosylamine-type oligosaccharides. NBD derivatives fluoresce by irradiating light at 470 nm. The maximum oscillation frequency of an argon ion laser is 488 nm. Therefore, a high sensitivity in LIF-CE using an argon laser was expected for NBD-labeled oligosaccharides.

Various modes have been proposed for the separation of labeled oligosaccharides by CE. These include plain capillary zone electrophoresis for size/charge resolution; micellar electrokinetic chromatography based on pseudo-partition chromatography; and borate complex mode for *in situ* formation of negatively charged borate complexes. We chose the borate complex mode in the

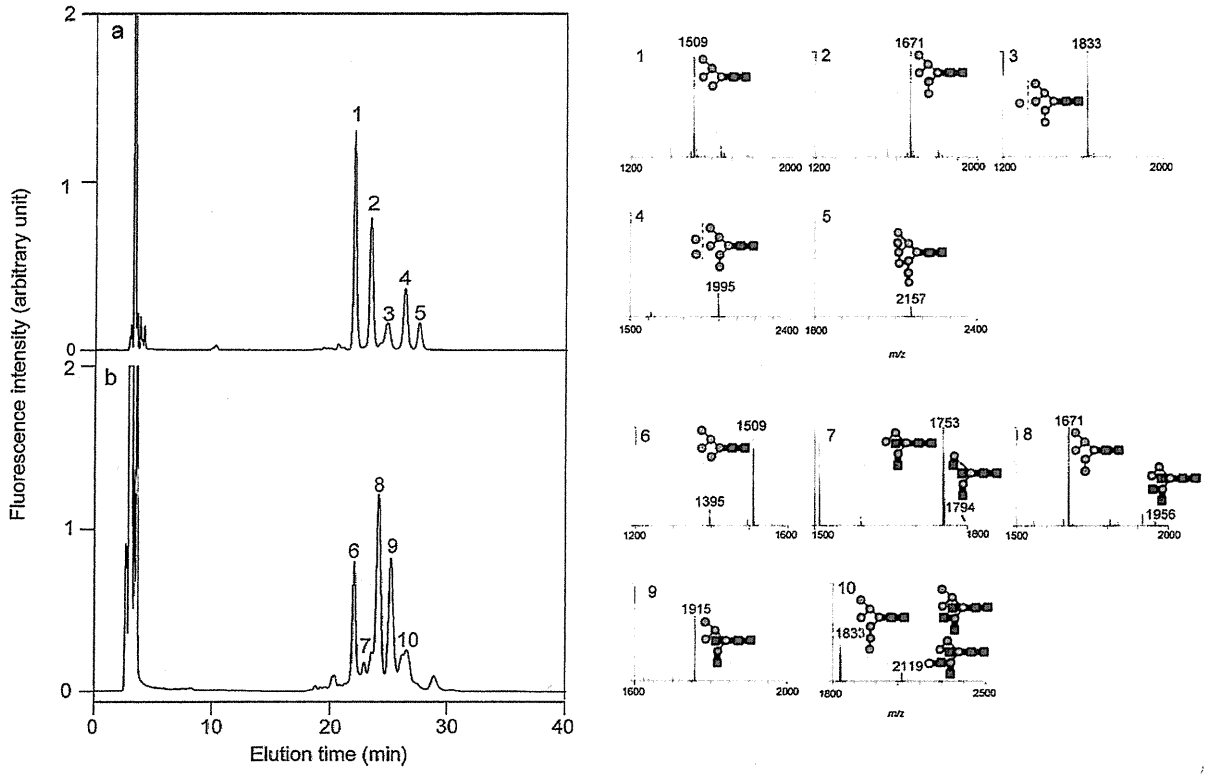

Fig. 5. Application of the PNGase F/NBD method for the HPLC analysis of oligosaccharides from bovine ribonuclease B (a) and ovalbumin (b). Analytical condition: column; Inertsil diol (4.6 mm × 250 mm), eluent; (A) 0.1% TFA, and (B) 95% acetonitrile containing 0.1% TFA, flow rate; 1.0 mL/min, gradient program; 99% (B) for 5 min, 99–75% (B) for 10 min, 75–50% (B) for 60 min, 50–1% (B) for 5 min, fluorometric detection; 470 nm (excitation)/540 nm (emission), amount of injection; 5 μg as a glycoprotein.

present study. NBD derivatives of oligosaccharides were separated as anionic borate complexes on neutrally coated capillary using 100 mM borate (pH 8.3) as the electrophoresis buffer. The neutrally coated capillary suppresses the generation of electroendoosmotic flow. Therefore, NBD-oligosaccharides move to the anode based on the number of acidic groups (*i.e.*, number of NeuAc residues) and the association with borate ions.

Fig. 6 shows the separation of NBD-labeled glycosylamine-type oligosaccharides derived from human transferrin, bovine fetuin, and human α_1-acid glycoprotein. Derivatives were separated based on the number of sialic acid residues. Tetrasialo-, trisialo- and disialooligosaccharides appeared at ~10–11 min, 12 min and 14 min, respectively. Further resolution seemed to be based on the difference in oligosaccharide structures. Transferrin-derived oligosaccharides indicated a large major peak corresponding to disialobiantennary oligosaccharides at 14 min, and small peaks observed at 14.2 min were assignable to fucosylated disialobiantennary oligosaccharides. Fetuin indicated two peaks each at tetrasialo-, trisialo- and disialooligosaccharide fractions. Splitting of the peaks at each fraction was probably due to the difference in linkage (*i.e.*, NeuAcα2 → 3 and NeuAcα2 → 6). These results showed very similar electropherograms to those of APTS-labeled oligosaccharides derived from fetuin [30]. Peak assignments shown in the figures were estimated from comparison of those electropherograms. As described above, α_1-acid glycoprotein contains biantennary, triantennary and tetraantennary oligosaccharides with 2–4 residues of NeuAc with or without fucose in one of the branches. Therefore, resolution of the oligosaccharides derived from this glycoprotein indicated a complex electropherogram. The limit of detection of NBD-labeled oligosaccharides was also estimated from a main peak of transferrin-derived oligosaccharides: it was 4 fmol (S/N ratio = 20).

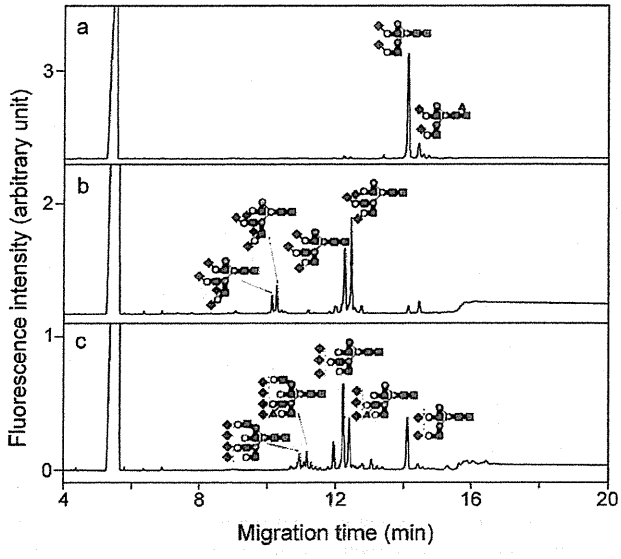

Fig. 6. Capillary electrophoresis with laser-induced fluorometric detection of oligosaccharides derived from human serum transferrin (a), fetal calf serum fetuin (b), and human α_1-acid glycoprotein (c). Analytical condition: capillary, InertCap® 1 (50 cm, 100 μm i.d.; effective length 40 cm); buffer, 100 mM borate (pH 8.3); capillary temperature, 25 °C; sample injection, 1 psi for 10 s; applied voltage, −15 kV.

4. Conclusion

The described method comprises digestion of PNGase F for the generation of glycosylamine-type oligosaccharides followed by fluorescent derivatization with NBD-F. This method has two

characteristic features: (i) sensitive analyses of *N*-linked oligosaccharide with easy operations attainable in a one-pot reaction within 3 h; and (ii) excitation maxima of NBD derivatives match LIF-CE using an argon laser. Sensitivity using fluorescence-detection HPLC was 4-times and 6-times higher than that previously reported for Fmoc- and ABEE-labeled oligosaccharides, respectively. The sensitivity of NBD derivatives in LC–ESI-MS was one order of magnitude higher than those labeled with ABEE and Fmoc. The sensitivity of NBD-labeled oligosaccharides was in the fmol range using LIF-CE. Therefore, the described method shows promise in the profiling of *N*-linked oligosaccharides in various biological samples as well as quality control in the manufacturing processes of glycoprotein pharmaceuticals.

Acknowledgments

This work was supported by the "High-Tech Research Center" Project for Private Universities: a matching fund subsidy from the Ministry of Education, Culture, Sports, Science and Technology (MEXT), Japan, 2007–2011.

References

[1] D.J. Harvey, J. Chromatogr. B (2010), doi:10.1016/j.jchromb.2010.11.010.
[2] S. Hase, T. Ikenaka, Y. Matsushima, Biochem. Biophys. Res. Commun. 85 (1978) 257.
[3] W.T. Wang, N.C. LeDonne Jr., B. Ackerman, C.C. Sweeley, Anal. Biochem. 141 (1984) 366.
[4] N. Tomiya, J. Awaya, M. Kurono, S. Endo, Y. Arata, N. Takahashi, Anal. Biochem. 171 (1988) 73.
[5] N. Takahashi, H. Nakagawa, K. Fujikawa, Y. Kawamura, N. Tomiya, Anal. Biochem. 226 (1995) 139.
[6] N. Takahashi, J. Chromatogr. A 720 (1996) 217.
[7] N. Takahashi, K. Kato, http://www.glycoanalysis.info/galaxy2/.
[8] A. Guttman, Nature 380 (1996) 461.
[9] F.T. Chen, R.A. Evangelista, Electrophoresis 19 (1998) 2639.
[10] T.S. Raju, J.B. Briggs, S.M. Borge, A.J. Jones, Glycobiology 10 (2000) 477.
[11] N. Callewaert, S. Geysens, F. Molemans, R. Conteras, Glycobiology 11 (2001) 275.
[12] F.-T.A. Chen, in: P. Thibault, S. Honda (Eds.), Methods Mol. Biol., Humana Press, 2002, p. 105.
[13] M. Yodoshi, A. Tani, Y. Ohta, S. Suzuki, J. Chromatogr. A 1203 (2008) 137.
[14] S. Kamoda, M. Nakano, R. Ishikawa, S. Suzuki, K. Kakehi, J. Proteome Res. 4 (2005) 146.
[15] R.A. Kekwick, R.K. Cannan, Biochem. J. 30 (1936) 227.
[16] T.H. Plummer Jr., J.H. Elder, S. Alexander, A.W. Phelan, A.L. Tarentino, J. Biol. Chem. 259 (1984) 10700.
[17] H.S. Isbell, H.L. Frush, J. Am. Chem. Soc. 72 (1950) 1043.
[18] Y. Satomi, Y. Shimonishi, T. Hase, T. Takao, Rapid. Commun. Mass Spectrom. 18 (2004) 2983.
[19] K. Imai, Y. Watanabe, Anal. Chim. Acta 130 (1981) 377.
[20] M.A. Bynum, H. Yin, K. Felts, Y.M. Lee, C.R. Monell, K. Killeen, Anal. Chem. 81 (2009) 8818.
[21] R.R. Townsend, M.R. Hardy, D.A. Cumming, J.P. Carver, B. Bendiak, Anal. Biochem. 182 (1989) 1.
[22] S. Suzuki, S. Honda, Electrophoresis 19 (1998) 2539.
[23] E.D. Green, G. Adelt, J.U. Baenziger, S. Wilson, H. Van Halbeek, J. Biol. Chem. 263 (1988) 18253.
[24] M. Nakano, K. Kakehi, M.H. Tsai, Y.C. Lee, Glycobiology 14 (2004) 431.
[25] B. Fournet, J. Montreuil, G. Strecker, L. Dorland, J. Haverkamp, J.F.G. Vliegenthart, P. Binette, K. Schmid, Biochemistry 17 (1978) 5206.
[26] A. Koller, J. Khandurina, J. Li, J. Kreps, D. Schieltz, A. Guttman, Electrophoresis 25 (2004) 2003.
[27] T. Tai, K. Yamashita, M. Ogata-Arakawa, N. Koide, T. Muramatsu, S. Iwashita, Y. Inoue, A. Kobata, J. Biol. Chem. 280 (1975) 8569.
[28] T. Tai, K. Yamashita, S. Ito, A. Kobata, J. Biol. Chem. 252 (1977) 6687.
[29] K. Yamashita, Y. Tachibana, A. Kobata, J. Biol. Chem. 253 (1978) 3862.
[30] A. Guttman, F.-T.A. Chen, R.A. Evangelista, Electrophoresis 17 (1996) 412.

Biochemical and Biophysical Research Communications 412 (2011) 50–54

Contents lists available at ScienceDirect

Biochemical and Biophysical Research Communications

journal homepage: www.elsevier.com/locate/ybbrc

HMG-CoA reductase inhibitor augments the serum total cholesterol-lowering effect of human adipose tissue-derived multilineage progenitor cells in hyperlipidemic homozygous Watanabe rabbits

Ayami Saga [a], Hanayuki Okura [a], Mayumi Soeda [a], Junko Tani [a], Yuichi Fumimoto [a], Hiroshi Komoda [a], Mariko Moriyama [a,b], Hiroyuki Moriyama [b], Shizuya Yamashita [c], Akihiro Ichinose [d], Takashi Daimon [e], Takao Hayakawa [b], Akifumi Matsuyama [a,*]

[a] Department of Somatic Stem Cell Therapy and Health Policy, Foundation for Biomedical Research and Innovation, TRI305, 1-5-4 Minatojima-minamimachi, Chuo-ku, Kobe, Hyogo 650-0047, Japan
[b] Pharmaceutical Research and Technology Institute, Kinki University, 3-4-1 Kowakae, Higashi-Osaka, Osaka 577-8502, Japan
[c] Division of Cardiology, Department of Internal Medicine, Osaka University Graduate School of Medicine, Suita, Osaka 565-0871, Japan
[d] Department of Plastic Surgery, Kobe University Hospital, 7-5-2 Kusunoki-cho, Chuo-ku, Kobe, Hyogo 660-0017, Japan
[e] Division of Biostatistics, Hyogo College of Medicine, 1-1 Mukogawa-cho, Nishinomiya, Hyogo 663-8501, Japan

ARTICLE INFO

Article history:
Received 7 July 2011
Available online 22 July 2011

Keywords:
ADMPC
WHHL
HMG-CoA reductase inhibitor
Pravastatin
Cholesterol
Cell therapy

ABSTRACT

Familial hypercholesterolemia (FH) is an autosomal codominant disease characterized by high concentrations of proatherogenic lipoproteins secondary to deficiency in low-density lipoprotein (LDL) receptor. We reported recently the use of *in situ* stem cell therapy of human adipose tissue-derived multilineage progenitor cells (hADMPCs) in lowering serum total cholesterol in the homozygous Watanabe heritable hyperlipidemic (WHHL) rabbits, an animal model of homozygous FH. Here we demonstrate that pravastatin, an HMG-CoA reductase inhibitor, augmented the cholesterol-lowering effect of transplanted hADMPCs and enhanced LDL clearance in homozygous WHHL rabbit. The results suggest the potential beneficial effects of *in situ* stem cell therapy in concert with appropriately selected pharmaceutical agents, in regenerative medicine.

1. Introduction

Familial hypercholesterolemia (FH) is characterized by premature and accelerated development of atherosclerotic lesions caused by elevated levels of cholesterol-rich lipoproteins in plasma. The disease is caused by mutations in the low-density lipoprotein (LDL) receptor gene that result in a significant decrease in receptor-mediated uptake of lipoproteins from the circulation [1–3]. Patients homozygous for defects in LDL receptors have serum cholesterol levels 5–10 times those of normal and suffer as early as the first two decades of life serious complications such as coronary artery disease [4,5]. In homozygous FH patients, conventional drug therapy such as HMG-CoA reductase inhibitors, collectively known as "statins", cannot treat the condition, and therapeutic recourses are limited to chronic plasmapheresis and orthotopic liver transplantation [1]. Although liver transplants lower LDL levels, the procedure is life threatening and, in addition, donor livers are in short supply. A number of gene therapy approaches have shown some promise in animal models and human [6–9]. As an alternative to whole-organ transplantation and/or gene therapy, cellular transplantation has been proposed to provide functional LDL receptors for the treatment of hypercholesterolemia. Transplantation of allogenic and xenogenic hepatocytes is reported to be effective in lowering serum cholesterol in the Watanabe heritable hyperlipidemic (WHHL) rabbit [10–13], which is an animal model of homozygous FH. In this context, we have reported the ability of human adipose tissue-derived multilineage progenitor cells (hADMPCs) to differentiate into hepatocytes both *in vitro* and *in vivo* and to rectify critical liver functions [14,15] similar to reports from other laboratories [16,17]. Various groups have demonstrated the *in vitro* differentiation of hADMPCs into various cell types and confirmed that hADMPCs can be easily and safely obtained in large quantities without serious ethical issues [14,15,18,19]. In homozygous FH patients, HMG-CoA reductase inhibitors have no effect on the condition as mentioned [20]. We hypothesized that HMG-CoA reductase inhibitor can act in concert with *in situ* differentiated hepatocyte-like cells originating from transplanted hADMPCs to lower serum cholesterol

* Corresponding author. Fax: +81 78 304 8707.
E-mail address: akifumi-matsuyama@umin.ac.jp (A. Matsuyama).

0006-291X/$ - see front matter © 2011 Elsevier Inc. All rights reserved.
doi:10.1016/j.bbrc.2011.07.035

levels in hyperlipidemia. To test our hypothesis, we tested the effects of treatment with HMG-CoA reductase inhibitor in hADMPC-transplanted homozygous WHHL rabbits.

2. Materials and methods

2.1. Adipose tissue samples

Subcutaneous adipose tissue samples (10–50 g, each) were resected during plastic surgery in 5 females (age, 20–60 years) as excess discards. The study protocol was approved by the Review Board for Human Research of Kobe University Graduate School of Medicine, Osaka University Graduate School of Medicine, Kinki University Pharmaceutical Research and Technology Institute and Foundation for Biomedical Research and Innovation. Each subject provided a signed informed consent.

2.2. isolation of hADMPCs

The hADMPCs were prepared as described previously [21] with some modification [14,15,18,19]. Briefly, the resected excess adipose tissue was minced and then digested at 37 °C for 1 h in Hank's balanced salt solution (HBSS, GIBCO Invitrogen, Grand Island, NY) containing 0.075% collagenase type I (Sigma Aldrich, St. Louis, MO). Digests were filtered through a cell strainer (BD Bioscience, San Jose, CA) and centrifuged at 800 *g* for 10 min. Erythrocytes were excluded using density gradient centrifugation with Lymphoprep ($d = 1.077$; Nycomed, Oslo, Norway), and the remaining cells were cultured in Dulbecco's modified Eagle's medium (DMEM, GIBCO Invitrogen) with 10% defined fetal bovine serum (FBS, GIBCO Invitrogen) for 24 h at 37 °C. Following incubation, the adherent cells were washed extensively and then treated with 0.2 g/l ethylenediaminetetraacetate (EDTA) solution (Nacalai Tesque, Kyoto, Japan). The resulting suspended cells were replated at a density of 10,000 cells/cm^2 on human fibronectin (FN)-coated dishes (AGC, Tokyo, Japan) in Stem Cell Medium (Nipro, Osaka, Japan), 1× insulin-transferring selenium (ITS, GIBCO Invitrogen), 1 nM dexamethasone (Sigma–Aldrich), 100 μM ascorbic acid 2-phosphate (Sigma Aldrich), 10 ng/ml epidermal growth factor (EGF, PeproTec, Rocky Hill, NJ), and 5% FBS (GIBCO Invitrogen). After 5–6 passages, the hADMPCs were used for transplantation.

2.3. hADMPCs transplantation and immunosuppression/statin treatment regimen

The transplantation procedure was performed as reported previously [15]. Briefly, 8-week-old homozygous WHHL rabbits (Kitayamalabes, Inc., Japan) ($n = 7$) were anesthetized with pentobarbital (50 mg/kg) and an incision distal and parallel to the lower end of the ribcage was made. The peritoneum was incised and hADMPCs (3×10^7 cells) suspended in 3 mL of HBSS (20 °C) with heparin were infused within 5 min into the portal vein via a 18-gauge Angiocath™ (BD, UT) (Fig. 1A). The immunosuppression regimen (Fig. 1B) consisted of the following: (i) intramuscular injection of cyclosporin A (6 mg/kg/day) daily from the day before surgery to sacrifice; (ii) intramuscular injection of rapamycin (0.05 mg/kg/day) daily from the day before surgery to sacrifice; (iii) methylprednisolone at 3 mg/kg/day (day −1 to 7), followed by tapering to 2 mg/kg/day (day 8–14), 1 mg/kg/day (day 15–21) and 0.5 mg/kg/day (day 22 to sacrifice); (iv) intravenous injection of cyclophosphamide (20 mg/kg/day) at day 0, 2, 5 and 7; (v) intramuscular injection of ganciclovir (2.5 mg/kg/day) was also administrated to avoid viral infection in the immunocompromised host. Twelve weeks after hADMPCs transplantation, the rabbits were divided into two groups; the first was treated with low dose pravastatin (0.75 mg/kg/day i.m., $n = 4$), an HMG-CoA reductase inhibitor (treatment group), while the second served as the control and injected intramuscularly with the vehicle ($n = 3$).

2.4. Assay for lipid profiling

Serum samples were obtained from nonfasting rabbits before and after pravastatin treatment (at 12 and 16 weeks). Serum total cholesterol and HDL-cholesterol fraction were measured using assay kits from Wako Pure Chemical Industries (Osaka, Japan)

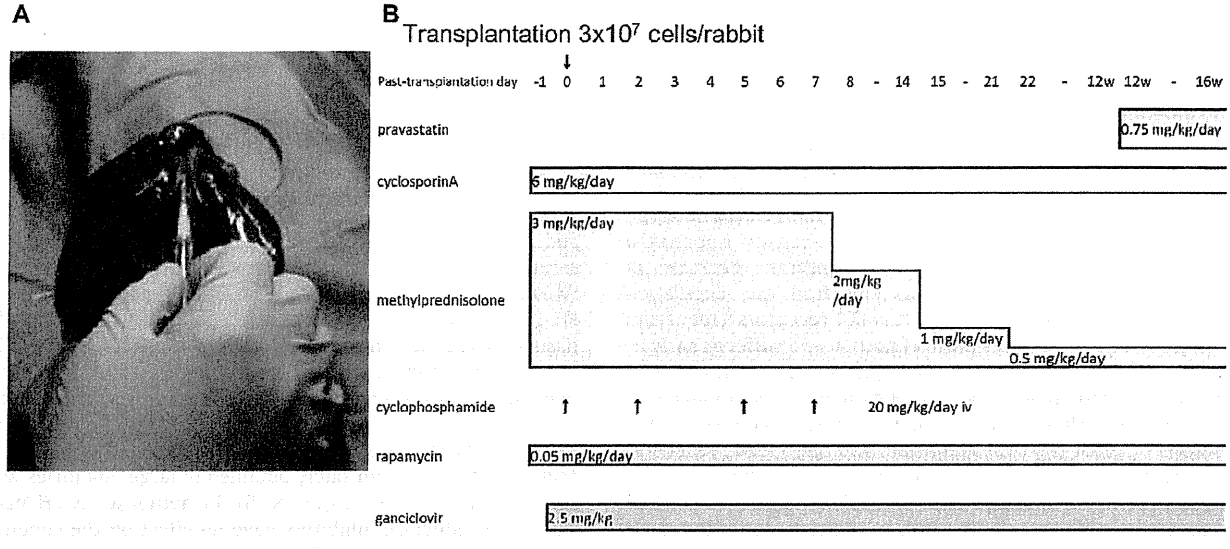

Fig. 1. (A) Surgical procedure. Watanabe heritable hyperlipidemic (WHHL) rabbits were anesthetized with pentobarbital. An incision was made distal and parallel to the lower end of the ribcage. The peritoneum was incised and hADMPCs (3×10^7 cells/rabbit) were infused into the portal vein using an 18-gauge Angiocath. (B) Immunosuppression regimen. Cyclosporin A (6 mg/kg/day) and rapamycin (0.05 mg/kg/day) were administered intramuscularly daily from the day before surgery to sacrifice. Methylprednisolone was administered at 3 mg/kg/day (days 1–7), 2 mg/kg/day (days 8–14), 1 mg/kg/day (days 15–21), and 0.5 mg/kg/day (day 22 to sacrifice). Cyclophosphamide (20 mg/kg/day) was injected intravenously at days 0, 2, 5, and 7. Ganciclovir (2.5 mg/kg/day) was also injected intramuscularly to avoid viral infection in the immunocompromised host. Twelve weeks after hADMPCs transplantation, hADMPC-transplanted WHHL rabbit were divided into two groups; the pravastatin-treated group ($n = 4$) and the control vehicle group ($n = 3$).

and the before and after treatment with/without pravastatin were compared in the two groups.

2.5. Clearance of ^{125}I-LDL from rabbit serum

LDL turnover study was performed as reported previously to examine the clearance of ^{125}I-LDL from rabbit serum [15]. Briefly, at the end of the study (Fig. 1B), the animals were examined for the LDL turnover assay. ^{125}I-human LDL (BT-913R, Biomedical Technologies Inc., Stoughton, MA) was delivered via the marginal ear vein of the WHHL rabbits and normal control rabbits in physiological saline containing 2 mg/mL bovine serum albumin. Blood was collected from the opposite ear after injection at 5 min, 1, 2, 3, 4, 6, 24 and 28 h. ^{125}I-labeled apolipoprotein B-containing LDL was precipitated with 20% of trichloroacetic acid (Wako Pure Chemical Industries) (serum; 320 μL, 100% w/v TCA 80 μL), and then the precipitants were applied for counting.

2.6. Statistical analysis

Values were expressed as mean ± SEM. Differences between mean values before and after treatment in the treated and untreated groups were evaluated using the paired *t*-test or Student's *t*-test. A *P* value less than 0.05 was considered statistically significant. All statistical analyses were performed using the SPSS Statistics 17.0 package (SPSS Inc., Chicago, IL).

3. Results

Pravastatin treatment significantly reduced serum total cholesterol level in hADMPC-transplanted homozygous WHHL rabbits ($n = 4$, before: 410 ± 35, after: 291 ± 46 mg/dL, $p = 0.0382$, Fig. 2), whereas control hADMPC-transplanted WHHL rabbits showed no such fall ($n = 3$, before: 409 ± 63, after: 375 ± 53 mg/dL, Fig. 2). On the other hand, the fall in HDL-cholesterol was not significant in both the pravastatin and control vehicle rabbits (pravastatin group: before 24.3 ± 0.5, after 23.3 ± 0.3 mg/dL, control vehicle group: before 22.8 ± 2.2, after 20.8 ± 2.2 mg/dL, Fig. 2).

Next, we measured human LDL clearance in order to confirm that the fall in serum total cholesterol induced by pravastatin in the hADMPCs-transplanted rabbits was mediated through human LDL receptors on hADMPC-derived hepatocytes (Fig. 3). Pravastatin shifted the LDL-turnover curve to the left ($n = 4$) (Fig. 3A). Furthermore, pravastatin significantly increased the 24-h LDL-clearance rate in the hADMPC-transplanted WHHL rabbits ($n = 4$, 95.0 ± 0.6%) compared to the control ($n = 3$, 90.7 ± 0.2%, $p = 0.0429$, Fig. 3).

4. Discussion

The main finding of this study was that pravastatin enhanced the lipid-lowering effects and the LDL-clearance rate of transplanted hADMPCs in spontaneously hyperlipidemic homozygous WHHL rabbits.

An important issue in cellular therapy is the cell source selected for clinical application. The major advantages of hADMPCs are their availability through simple harvesting surgical procedure and lack of ethical obstacles. In fact, a simple liposuction surgery yields massive amount of lipoaspirate adipose tissue, ranging from 100 ml to >3 L [22]. Our previous study in homozygous WHHL rabbits showed that human LDL binds to the receptors on hADMPC-derived hepatocytes and such human LDL receptors compensate the non-functional mutant LDL receptors in the WHHL rabbit [15]. Moreover, hepatocytes derived from hADMPCs have the advantage of expressing LDL receptor from an endogenous gene with intact regulatory sequences. These findings prompted us to test the effect of HMG-CoA reductase inhibitor on serum total cholesterol in hyperlipidemic rabbits transplanted with hADMPCs.

Among the numerous enzymes involved in the cholesterol biosynthesis pathway, HMG-CoA reductase plays an essential in cholesterol synthesis. Inhibition of the HMG-CoA enzyme by pravastatin decreases LDL-cholesterol by the following mechanisms: *de novo* decrease in cholesterol synthesis, simultaneous increase in

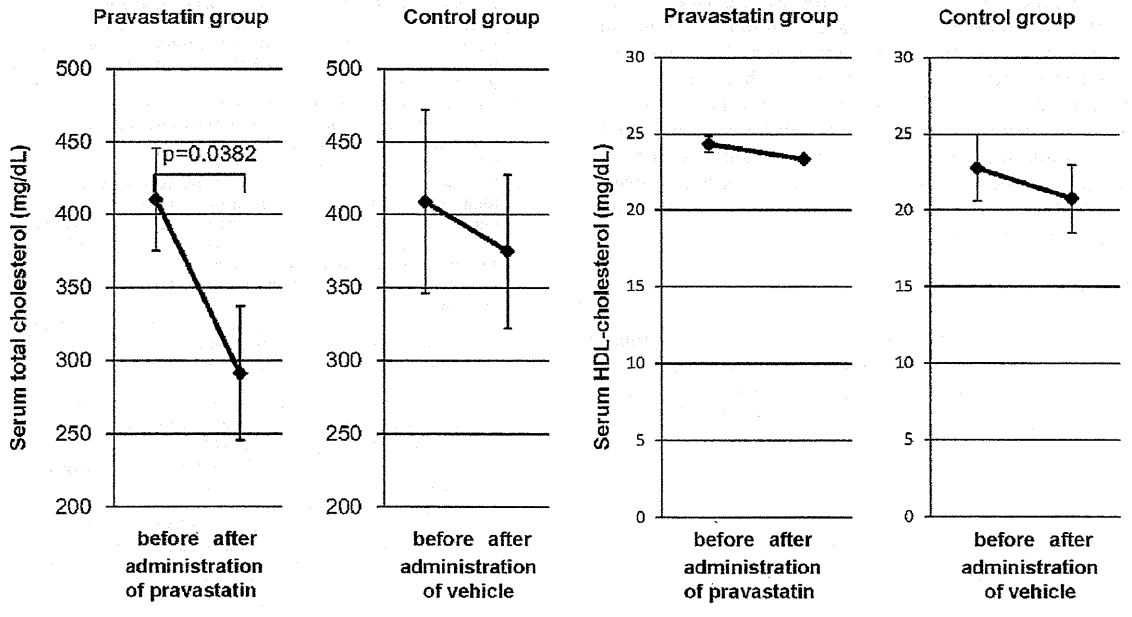

Fig. 2. Serum total cholesterol (*left*) and serum HDL-cholesterol (*right*) in hADMPC-transplanted homozygous WHHL rabbits before and after administration of pravastatin ($n = 4$) or the vehicle ($n = 3$). Data are mean ± SEM. Differences between mean values before and after administration of in the pravastatin or the vehicle were evaluated using the paired *t*-test. A *P* value less than 0.05 was considered statistically significant.

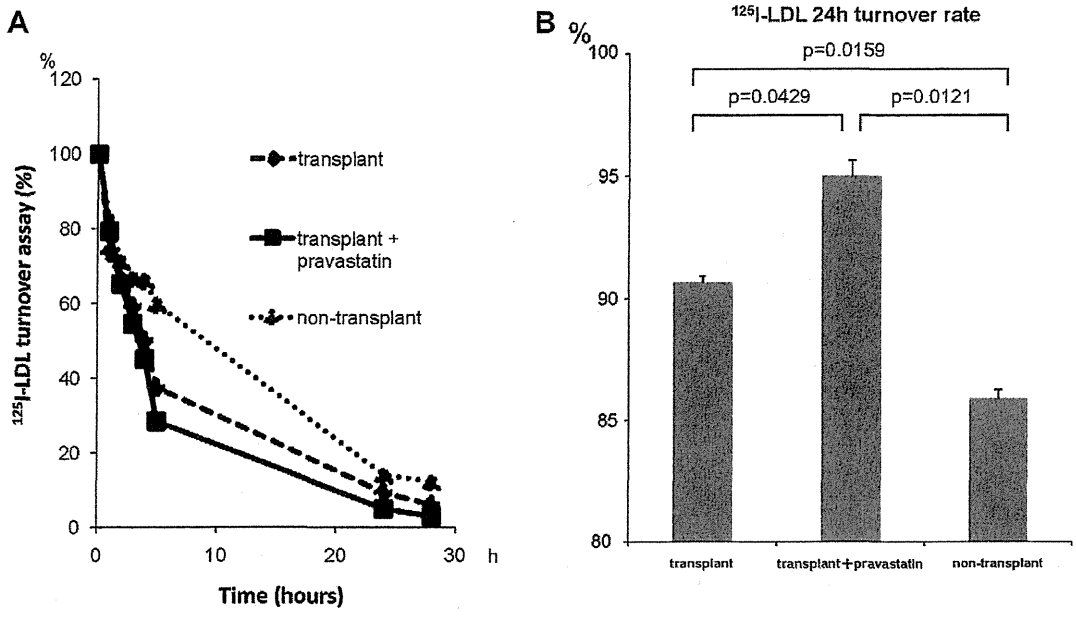

Fig. 3. (A) Rate of clearance of LDL from the serum of WHHL rabbits with and without transplantation of hADMPCs. Animals were injected with ^{125}I-labeled human LDL, and the time course of clearance was monitored following trichloroacetic acid precipitation of serum at time 5 min, 1 h, 2 h, 4 h, 6 h, 24 h and 28 h. Residual ^{125}I-LDL was expressed as percentage of that at 5 min. (B) Differences in the 24-h LDL-clearance rate in pravastatin-treated hADMPC-transplanted group ($n = 4$), hADMPC-transplanted control group ($n = 3$), and non-transplanted control homozygous WHHL group ($n = 3$). Data are mean ± SEM. Differences between mean values before and after treatment in the treated and untreated groups were evaluated using the Student's t-test. A P value less than 0.05 was considered statistically significant.

the LDL receptor synthesis on hepatocytes, thus enhancing the clearance of LDL-cholesterol from the circulation, resulting in lowering serum cholesterol levels [20]. For these reason, pravastatin fail to act in patients with homozygous FH who have no LDL receptor due to the genetic abnormality, and also in the homozygous hyperlipidemic WHHL rabbit, in which pravastatin could show cholesterol-lowering effects in much higher doses of 50 mg/kg/day [23–26]. The substantial fall in serum cholesterol and increased LDL-clearance from the circulation by pravastatin noted in the present study suggest that the hADMPC-derived hepatocyte-like cells both internalize LDL and metabolize cholesterol more efficiently and in concert with pravastatin. The relationship between hypercholesterolemia and coronary heart disease has been well documented, and a reduction in serum total cholesterol of the magnitude demonstrated in the present study is likely to reduce morbidity and mortality rates in patients with homozygous FH [27]. Further studies are needed to tests the potential usefulness of hADMPC-transplantation and simultaneous treatment pravastatin in these patients.

Acknowledgments

This study was supported in part by the Program for Promotion of Fundamental Studies in Health Sciences of the National Institute of Biomedical Innovation (NIBIO), and Kobe Translational Research Cluster, the Knowledge Cluster Initiative, Ministry of Education, Culture, Sports, Science and Technology (MEXT).

References

[1] M.S. Brown, J.L. Goldstein, A receptor-mediated pathway for cholesterol homeostasis, Science 232 (1986) 34–47.
[2] R.J. Havel, N. Yamada, D.M. Shames, Watanabe heritable hyperlipidemic rabbit. Animal model for familial hypercholesterolemia, Arteriosclerosis 9 (1) (1989) 133–138.
[3] T. Yamamoto, R.W. Bishop, M.S. Brown, J.L. Goldstein, D.W. Russell, Deletion in cysteine-rich region of LDL receptor impedes transport to cell surface in WHHL rabbit, Science 32 (1986) 1230–1237.
[4] T. Maruyama, S. Yamashita, Y. Matsuzawa, H. Bujo, K. Takahashi, Y. Saito, S. Ishibashi, K. Ohashi, F. Shionoiri, T. Gotoda, N. Yamada, T. Kita, Research Committee on Primary Hyperlipidemia of the Ministry of Health and Welfare of Japan. Mutations in Japanese subjects with primary hyperlipidemia – results from the Research Committee of the Ministry of Health and Welfare of Japan since 1996, J. Atheroscler. Thromb. 11 (2004) 131–145.
[5] S. Yamashita, H. Bujo, H. Arai, M. Harada-Shiba, S. Matsui, M. Fukushima, Y. Saito, T. Kita, Y. Matsuzawa, Long-term probucol treatment prevents secondary cardiovascular events: a cohort study of patients with heterozygous familial hypercholesterolemia in Japan, J. Atheroscler. Thromb. 15 (2008) 292–303.
[6] J.R. Chowdhury, M. Grossman, S. Gupta, N.R. Chowdhury, J.R. Baker Jr., J.M. Wilson, Long-term improvement of hypercholesterolemia after ex vivo gene therapy in LDLR-deficient rabbits, Science 254 (1991) 1802–1805.
[7] S. Ishibashi, M.S. Brown, J.L. Goldstein, R.D. Gerard, R.E. Hammer, J. Herz, Hypercholesterolemia in low density lipoprotein receptor knockout mice and its reversal by adenovirus-mediated gene delivery, J. Clin. Invest. 92 (1993) 883–893.
[8] K.F. Kozarsky, D.R. McKinley, L.L. Austin, S.E. Raper, L.D. Stratford-Perricaudet, J.M. Wilson, In vivo correction of low density lipoprotein receptor deficiency in the Watanabe heritable hyperlipidemic rabbit with recombinant adenoviruses, J. Biol. Chem. 269 (1994) 13695–13702.
[9] J.M. Wilson, N.R. Chowdhury, M. Grossman, R. Wajsman, A. Epstein, R.C. Mulligan, J.R. Chowdhury, Temporary amelioration of hyperlipidemia in low density lipoprotein receptor-deficient rabbits transplanted with genetically modified hepatocytes, Proc. Natl. Acad. Sci. USA 87 (1990) 8437–8441.
[10] J.R. Gunsalus, D.A. Brady, S.M. Coulter, B.M. Gray, A.S. Edge, Reduction of serum cholesterol in Watanabe rabbits by xenogeneic hepatocellular transplantation, Nat. Med. 3 (1997) 48–53.
[11] M.L. Tejera, J.A. Cienfuegos, P. Maganto, F. Pardo, L. Santamaria, J. Codesal, S. De Andres, J.L. Hernandez, J.L. Castillo-Olivares, Reduction of cholesterol levels following liver cell grafting in hyperlipidemic (WHHL) rabbits, Transplant. Proc. 24 (1992) 160–161.
[12] J. Wang, R. Pollak, A. Bartholomew, Sustained reduction of serum cholesterol levels following allo-transplantation of parenchymal hepatocytes in Watanabe rabbits, Transplant. Proc. 23 (1991) 894–895.
[13] J.C. Wiederkehr, G.T. Kondos, R. Pollak, Hepatocyte transplantation for the low-density lipoprotein receptor-deficient state. A study in the Watanabe rabbit, Transplantation 50 (1990) 466–471.
[14] H. Okura, H. Komoda, A. Saga, A. Kakuta-Yamamoto, Y. Hamada, Y. Fumimoto, C.M. Lee, A. Ichinose, Y. Sawa, A. Matsuyama, Properties of hepatocyte-like cell clusters from human adipose tissue-derived mesenchymal stem cells, Tissue Eng. Part C Methods 16 (2010) 761–770.
[15] H. Okura, A. Saga, Y. Fumimoto, M. Soeda, M. Moriyama, H. Moriyama, K. Nagai, C.M. Lee, S. Yamashita, A. Ichinose, T. Hayamakawa, A. Matsuyama, Transplantation of human adipose tissue-derived multilineage progenitor cells reduces serum cholesterol in hyperlipidemic Watanabe rabbits, Tissue Eng. Part C Methods 17 (2011) 145–154.

[16] M.J. Seo, S.Y. Suh, Y.C. Bae, J.S. Jung, Differentiation of human adipose stromal cells into hepatic lineage in vitro and in vivo, Biochem. Biophys. Res. Commun. 328 (2005) 258–264.

[17] A. Banas, T. Teratani, Y. Yamamoto, M. Tokuhara, F. Takeshita, G. Quinn, H. Okochi, T. Ochiya, Adipose tissue-derived mesenchymal stem cells as a source of human hepatocytes, Hepatology 46 (2007) 219–228.

[18] H. Komoda, H. Okura, C.M. Lee, N. Sougawa, T. Iwayama, T. Hashikawa, A. Saga, A. Yamamoto, A. Ichinose, S. Murakami, Y. Sawa, A. Matsuyama, Reduction of Nglycolylneuraminic acid xenoantigen on human adipose tissue-derived stromal cells/mesenchymal stem cells leads to safer and more useful cell sources for various stem cell therapies, Tissue Eng. Part A 16 (2010) 1143–1155.

[19] H. Okura, A. Matsuyama, C.M. Lee, A. Saga, A. Kakuta-Yamamoto, A. Nagao, N. Sougawa, N. Sekiya, K. Takekita, Y. Shudo, S. Miyagawa, H. Komoda, T. Okano, Y. Sawa, Cardiomyoblast-like cells differentiated from human adipose tissue-derived mesenchymal stem cells improve left ventricular dysfunction and survival in a rat myocardial infarction model, Tissue Eng. Part C Methods 16 (2010) 417–425.

[20] S. Nozaki, T. Nakagawa, A. Nakata, S. Yamashita, K. Kameda-Takemura, T. Nakamura, Y. Keno, K. Tokunaga, Y. Matsuzawa, Effects of pravastatin on plasma and urinary mevalonate concentrations in subjects with familial hypercholesterolaemia: a comparison of morning and evening administration, Eur. J. Clin. Pharmacol. 49 (1996) 361–364.

[21] P. Bjorntorp, M. Karlsson, H. Pertoft, P. Pettersson, L. Sjostrom, U. Smith, Isolation and characterization of cells from rat adipose tissue developing into adipocytes, J. Lipid Res. 19 (1978) 316–324.

[22] J.M. Gimble, A.J. Katz, B.A. Bunnell, Adipose-derived stem cells for regenerative medicine, Circ. Res. 100 (2007) 1249–1260.

[23] F.J. Dowell, C.A. Hamilton, G.B. Lindop, J.L. Reid, Development and progression of atherosclerosis in aorta from heterozygous and homozygous WHHL rabbits. Effects of simvastatin treatment, Arterioscler. Thromb. Vasc. Biol. 15 (1995) 1152–1160.

[24] M. Harsch, A. Gebhardt, A. Reymann, G. Lang, M. Schliack, R. Löser, J.H. Braesen, A. Niendorf, Effects of pravastatin on cholesterol metabolism of cholesterol-fed heterozygous WHHL rabbits, Br. J. Pharmacol. 124 (1998) 277–282.

[25] M. Kuroda, A. Matsumoto, H. Itakura, Y. Watanabe, T. Ito, M. Shiomi, J. Fukushige, F. Nara, M. Fukami, Y. Tsujita, Effects of pravastatin sodium alone and in combination with cholestyramine on hepatic, intestinal and adrenal low density lipoprotein receptors in homozygous Watanabe heritable hyperlipidemic rabbits, Jpn. J. Pharmacol. 59 (1992) 65–70.

[26] M. Shiomi, T. Ito, Y. Watanabe, Y. Tsujita, M. Kuroda, M. Arai, M. Fukami, J. Fukushige, A. Tamura, Suppression of established atherosclerosis and xanthomas in mature WHHL rabbit by keeping their serum cholesterol levels extremely low. Effect of pravastatin sodium in combination with cholestyramine, Atherosclerosis 83 (1990) 69–80.

[27] D. Steinberg, J.L. Witztum, Current concepts. Lipoproteins and atherogenesis, JAMA 264 (1990) 3047–3052.

Efficient and Directive Generation of Two Distinct Endoderm Lineages from Human ESCs and iPSCs by Differentiation Stage-Specific SOX17 Transduction

Kazuo Takayama[1,2], Mitsuru Inamura[1,2], Kenji Kawabata[2,3], Katsuhisa Tashiro[2], Kazufumi Katayama[1], Fuminori Sakurai[1], Takao Hayakawa[4,5], Miho Kusuda Furue[6,7], Hiroyuki Mizuguchi[1,2,8]*

1 Laboratory of Biochemistry and Molecular Biology, Graduate School of Pharmaceutical Sciences, Osaka University, Suita, Osaka, Japan, **2** Laboratory of Stem Cell Regulation, National Institute of Biomedical Innovation, Ibaraki, Osaka, Japan, **3** Laboratory of Biomedical Innovation, Graduate School of Pharmaceutical Sciences, Osaka University, Suita, Osaka, Japan, **4** Pharmaceutics and Medical Devices Agency, Chiyoda-ku, Tokyo, Japan, **5** Pharmaceutical Research and Technology Institute, Kinki University, Higashiosaka, Osaka, Japan, **6** JCRB Cell Bank, Division of Bioresources, National Institute of Biomedical Innovation, Ibaraki, Osaka, Japan, **7** Laboratory of Cell Processing, Institute for Frontier Medical Sciences, Kyoto University, Sakyo-ku, Kyoto, Japan, **8** The Center for Advanced Medical Engineering and Informatics, Osaka University, Suita, Osaka, Japan

Abstract

The establishment of methods for directive differentiation from human embryonic stem cells (ESCs) and induced pluripotent stem cells (iPSCs) is important for regenerative medicine. Although Sry-related HMG box 17 (SOX17) overexpression in ESCs leads to differentiation of either extraembryonic or definitive endoderm cells, respectively, the mechanism of these distinct results remains unknown. Therefore, we utilized a transient adenovirus vector-mediated overexpression system to mimic the SOX17 expression pattern of embryogenesis. The number of alpha-fetoprotein-positive extraembryonic endoderm (ExEn) cells was increased by transient SOX17 transduction in human ESC- and iPSC-derived primitive endoderm cells. In contrast, the number of hematopoietically expressed homeobox (HEX)-positive definitive endoderm (DE) cells, which correspond to the anterior DE *in vivo*, was increased by transient adenovirus vector-mediated SOX17 expression in human ESC- and iPSC-derived mesendoderm cells. Moreover, hepatocyte-like cells were efficiently generated by sequential transduction of SOX17 and HEX. Our findings show that a stage-specific transduction of SOX17 in the primitive endoderm or mesendoderm promotes directive ExEn or DE differentiation by SOX17 transduction, respectively.

Citation: Takayama K, Inamura M, Kawabata K, Tashiro K, Katayama K, et al. (2011) Efficient and Directive Generation of Two Distinct Endoderm Lineages from Human ESCs and iPSCs by Differentiation Stage-Specific SOX17 Transduction. PLoS ONE 6(7): e21780. doi:10.1371/journal.pone.0021780

Editor: Patrick Callaerts, VIB & Katholieke Universiteit Leuven, Belgium

Received February 3, 2011; **Accepted** June 8, 2011; **Published** July 7, 2011

Funding: HM, MKF, and TH were supported by grants from the Ministry of Health, Labor, and Welfare of Japan. K. Kawabata was supported by grants from the Ministry of Education, Sports, Science and Technology of Japan (20200076) and the Ministry of Health, Labor, and Welfare of Japan. K. Katayama was supported by the Program for Promotion of Fundamental Studies in Health Sciences of the National Institute of Biomedical Innovation (NIBIO). The funders had no role in study design, data collection and analysis, decision to publish, or preparation of the manuscript.

Competing Interests: The authors have declared that no competing interests exist.

* E-mail: mizuguch@phs.osaka-u.ac.jp

Introduction

There are two distinct endoderm lineages in early embryogenesis, the extraembryonic endoderm (ExEn) and the definitive endoderm (DE). The first of these lineages, the ExEn plays crucial roles in mammalian development, although it does not contribute to the formation of body cells. In early embryogenesis, a part of the inner cell mass of the blastocyst differentiates into the primitive endoderm (PrE). The PrE differentiates into the ExEn that composes the parietal endoderm, which contributes to the primary yolk sac, and the visceral endoderm, which overlies the epiblast [1,2]. In contrast, the second of the endoderm lineages, the DE arises from the primitive streak (PS), which is called the mesendoderm [3]. The DE has the ability to differentiate into the hepatic and pancreatic tissue [4].

The establishment of human embryonic stem cells (ESCs) [5] and human induced pluripotent stem cells (iPSCs) [6,7] has opened up new opportunities for basic research and regenerative medicine. To exploit the potential of human ESCs and iPSCs, it is necessary to understand the mechanisms of their differentiation. Although growth factor-mediated ExEn or DE differentiation is widely performed, it leads to a heterogeneous population [8,9,10,11]. Several studies have utilized not only growth factors but also modulation of transcription factors to control downstream signaling cascades [10,12,13]. Sox17, an Sry-related HMG box transcription factor, is required for development of both the ExEn and DE. In mice, during ExEn and DE development, Sox17 expression is first observed in the PrE and in the anterior PS, respectively [14]. Previous study showed that stable Sox17 overexpression promotes ExEn differentiation from mouse ESCs [12]. On the other hand, another previous study has demonstrated that DE progenitors can be established from human ESCs by stable expression of SOX17 [10]. The mechanism of these discrepancies which occurs in SOX17 transduction still remains unknown. Also, the role of SOX17 in human ExEn differentiation still remains unknown. Therefore, it is quite difficult to promote directive differentiation into either ExEn or DE cells by SOX17 transduction.

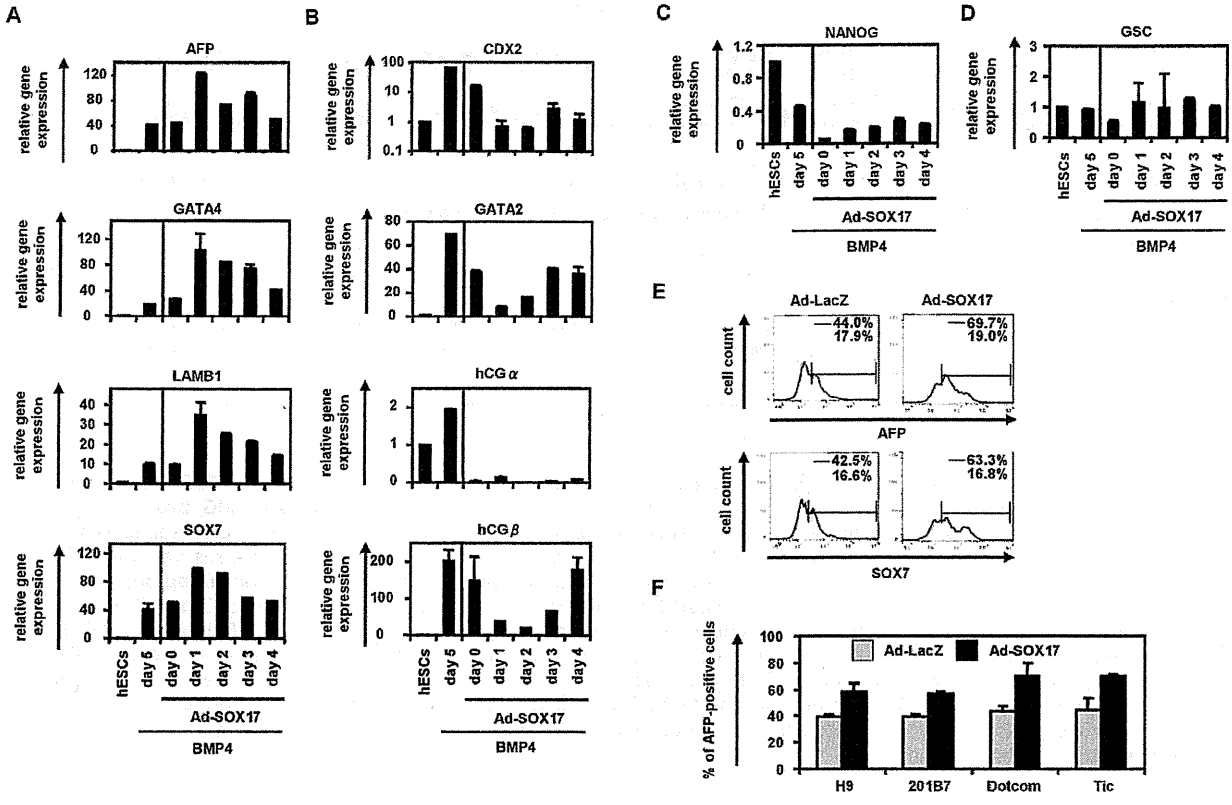

Figure 1. Efficient ExEn differentiation from human ESC- and iPSC-derived PrE cells by SOX17 transduction. (A–D) Undifferentiated human ESCs (H9) and BMP4-induced human ESC-derived cells, which were cultured with the medium containing BMP4 (20 ng/ml) for 0, 1, 2, 3, and 4 days, were transduced with 3,000 VP/cell of Ad-SOX17 for 1.5 h. Ad-SOX17-transduced cells were cultured with 20 ng/ml of BMP4, and then the gene expression levels of *(A)* the ExEn markers (AFP, GATA4, LAMB1, and SOX7), (B) the trophectoderm markers (CDX2, GATA2, hCGα, and hCGβ), (C) the pluripotent marker (NANOG), and (D) the DE marker (GSC) were examined by real-time RT-PCR on day 5 of differentiation. The horizontal axis represents the day on which the cells were transduced with Ad-SOX17. The expression levels of undifferentiated human ESCs on day 0 were defined 1.0. (E) On day 1, human ESC-derived PrE cells, which were cultured with the medium containing BMP4 for 1 day, were transduced with Ad-LacZ or Ad-SOX17 and cultured until day 5. The ExEn cells were subjected to immunostaining with anti-AFP or anti-SOX7 antibodies, and then analyzed by flow cytometry. (F) After Ad-LacZ or Ad-SOX17 transduction, the efficacies of ExEn differentiation from the human ES cell line (H9) and the three human iPS cell lines (201B7, Dotcom, and Tic) were compared on day 5 of differentiation. All data are represented as the means±SD ($n=3$).
doi:10.1371/journal.pone.0021780.g001

In this study, we utilized SOX17 as a stage-specific regulator of ExEn and DE differentiation from human ESCs and iPSCs. The human ESC- and iPSC-derived cells were transduced with SOX17-expressing adenovirus vector (Ad-SOX17), and the resulting phenotypes were assessed for their ability to differentiate into ExEn and DE cells *in vitro*. In addition, we examined whether SOX17-transduced cells have the ability to differentiate into the hepatic lineage. The results showed that stage-specific overexpression of the SOX17 transcription factor promotes directive differentiation into either ExEn or DE cells.

Results

The induction of human ESC-derived PrE cells and human ESC-derived mesendoderm cells

To determine the appropriate stage for SOX17 transduction, ExEn or DE cells were differentiated from human ESCs by a conventional method using BMP4 (20 ng/ml) or Activin A (100 ng/ml), respectively (Figures S1 and S2). Experiments for bidirectional differentiation using BMP4 and Activin A indicated that PrE cells were obtained on day 1 (Figure S1) and mesendoderm cells were obtained on day 3 (Figure S2). We expected that stage-specific SOX17 transduction into PrE cells or mesendoderm cells could promote ExEn or DE differentiation, because the time period of intiation of SOX17 expression was correlated with the time period of formation of PrE cells (day 1) (Figure S1C) and mesendoderm cells (day 3) (Figure S2C), respectively.

PrE stage-specific SOX17 overexpression promotes directive ExEn differentiation from human ESCs

To examine the effect of forced and transient expression of SOX17 on the differentiation of human ESC- and iPSC-derived cells, we used a fiber-modified adenovirus (Ad) vector containing the EF-1α promoter and a stretch of lysine residues (KKKKKKK, K7) peptides in the C-terminal region of the fiber knob. The K7 peptide targets heparan sulfates on the cellular surface, and the fiber-modified Ad vector containing the K7 peptides has been shown to be efficient for transduction into many kinds of cells [15,16].

Because the time period of initiation of SOX17 expression was correlated with the time period of formation of PrE cells (day 1) (Figure S1), we expected that stage-specific SOX17 transduction

into PrE cells would promote ExEn differentiation. Therefore, we examined the stage-specific role of SOX17 in ExEn differentiation. Ad-SOX17 transduction was performed in human ESCs treated with BMP4 for 0, 1, 2, 3, or 4 days, and the Ad-SOX17-transduced cells were cultured with medium containing BMP4 until day 5 (Figures 1A–1D). We confirmed the expression of exogenous SOX17 in the human ESC-derived mesendoderm cells transduced with Ad-SOX17 (Figure S3). Since BMP4 is known for its capability to induce both ExEn and trophectoderm [8,9], we analyzed not only the expression levels of ExEn markers but also those of trophectoderm markers by real-time RT-PCR after 5 days of differentiation (Figures 1A and 1B). The transduction of Ad-SOX17 on day 1 led to the highest expression levels of ExEn markers, alpha-fetoprotein (AFP), GATA4, laminin B1 (LAMB1), and SOX7 [17,18,19]. In contrast, the expression levels of the trophectoderm markers CDX2, GATA2, hCGα (human chorionic gonadotropin), and hCGβ [20] were down-regulated in Ad-SOX17-transduced cells as compared with non-transduced cells (Figure 1B). The expression levels of the pluripotent marker NANOG and DE marker GSC were not increased by SOX17 transduction (Figures 1C and 1D). We confirmed that there were no differences between non-transduced cells and Ad-LacZ-transduced cells in gene expression levels of all the markers investigated in Figures 1A–1D (data not shown). Therefore, we concluded that ExEn cells were efficiently induced from Ad-SOX17-transduced PrE cells.

The effects of SOX17 transduction on the ExEn differentiation from human ESC-derived PrE cells were also assessed by quantifying AFP- or SOX7-positive ExEn cells. The percentage of AFP- or SOX7-positive cells was significantly increased in Ad-SOX17-transduced cells (69.7% and 63.3%, respectively) (Figure 1E). Similar results were observed in the human iPS cell lines (201B7, Dotcom, and Tic) (Figure 1F). These findings indicated that stage-specific SOX17 overexpression in human ESC-derived PrE cells enhances ExEn differentiation.

Mesendoderm stage-specific SOX17 overexpression promotes directive DE differentiation from human ESCs

To examine the effects of transient SOX17 overexpression on DE differentiation from human ESCs, we optimized the timing of the Ad-SOX17 transduction. Ad-SOX17 transduction was performed in human ESCs treated with Activin A (100 ng/ml) for 0, 1, 2, 3, or 4 days, and the Ad-SOX17-transduced cells were cultured with medium containing Activin A (100 ng/ml) until day 5 (Figures 2A–2C). Using a fiber-modified Ad vector, both undifferentiated human ESCs and Activin A-induced human ESC-derived cells were efficiently transduced (Figure S4). The transduction of SOX17 on day 3 led to the highest expression levels of the DE markers FOXA2 [21], GSC [22], GATA4 [17], and HEX [23] (Figure 2A). In contrast to the DE markers, the expression levels of the pluripotent marker NANOG [24] were down-regulated in Ad-SOX17-transduced cells as compared with non-transduced cells (Figure 2B). The expression levels of the ExEn marker SOX7 [14] were up-regulated, when Ad-SOX17 transduction was performed into human ESCs treated with Activin A (100 ng/ml) for 0, 1, or 2 days (Figure 2C). On the other hand, the expression levels of the ExEn marker SOX7 were significantly down-regulated, when Ad-SOX17 transduction was performed into human ESCs treated with Activin A (100 ng/ml) for 3 or 4 days, indicating that SOX17 overexpression prior to mesendoderm formation (day 0, 1, and 2) promoted not only DE differentiation but also ExEn differentiation. Similar results were obtained with the human iPS cell line (Tic) (Figure S5). Although the expression levels of the mesoderm marker FLK1 [25] did not exhibit any change when Ad-SOX17 transduction was performed into human ESCs treated with Activin A (100 ng/ml) for 0, 1, or 2 days (Figure 2D), their expression levels were significantly down-regulated when Ad-SOX17 transduction was performed into human ESCs treated with Activin A (100 ng/ml) for 3 or 4 days. These results suggest that SOX17 overexpression promotes directive differentiation from mesendoderm cells into the DE cells, but not into mesoderm cells. We also confirmed that Ad-vector mediated gene expression in the human ESC-derived mesendoderm cells (day 3) continued until day 6 and disappeared on day 10 (Figure S6). SOX17 transduction in the human ESC-derived cells on day 3 and 4 had no effect on cell viability, while that in the cells on day 0, 1, and 2 resulted in severely impaired cell viability (Figure S7), probably because SOX17 transduction directed the cells on day 0, 1, and 2 to differentiate into ExEn cells but the medium containing Activin A (100 ng/ml) was inappropriate for ExEn cells. We confirmed that there were no differences between non-transduced cells and Ad-LacZ-transduced cells in gene expression levels of all the markers investigated in Figures 2A–2D (data not shown). These results indicated that stage-specific SOX17 overexpression in human ESC-derived mesendoderm cells is essential for promoting efficient DE differentiation.

It has been previously reported that human ESC-derived mesendoderm cells and DE cells became CXCR4-positive (>80%) by culturing human ESCs with Activin A (100 ng/ml) [26]. However, Activin A is not sufficient for homogenous differentiation of c-Kit/CXCR4-double-positive DE cells [10,11] or HEX-positive anterior DE cells [23]. Seguin et al. and Morrison et al. reported that the differentiation efficiency of c-Kit/CXCR4-double-positive DE cells was approximately 30% in the absence of stable Sox17 expression and that of HEX-positive anterior DE cells was only about 10% [10,23]. Therefore, we next examined whether Ad-SOX17 transduction improves the differentiation efficiency of c-Kit/CXCR4-double-positive DE cells and HEX-positive anterior DE cells. Human ESC-derived mesendoderm cells were transduced with Ad-SOX17, and the number of CXCR4/c-Kit-double-positive cells was analyzed by using a flow cytometer. The percentage of CXCR4/c-Kit-double-positive cells was significantly increased in Ad-SOX17-transduced cells (67.7%), while that in Ad-LacZ-transduced cells was only 22% (Figure 2E). The percentage of HEX-positive cells was also significantly increased in Ad-SOX17-transduced cells (53.7%), while that in Ad-LacZ-transduced cells was approximately 11% (Figure 2F). Similar results were also observed in the three human iPS cell lines (201B7, Dotcom, and Tic) (Figure 2G). These findings indicated that stage-specific SOX17 overexpression in human ESC-derived mesendoderm cells promotes efficient differentiation of DE cells.

Ad-SOX17-transduced cells tend to differentiate into the hepatic lineage

To investigate whether Ad-SOX17-transduced cells have the ability to differentiate into hepatoblasts and hepatocyte-like cells, Ad-SOX17-transduced cells were differentiated according to our previously described method [13]. Our previous report demonstrated that transient HEX transduction efficiently generates hepatoblasts from human ESC- and iPSC-derived DE cells. The hepatic differentiation protocol used in this study is illustrated in Figure 3A. After the hepatic differentiation, the morphology of human ESCs transduced with Ad-SOX17 followed by Ad-HEX was gradually changed into a hepatocyte morphology: polygonal in shape with distinct round nuclei by day 18 (Figure 3B). We also